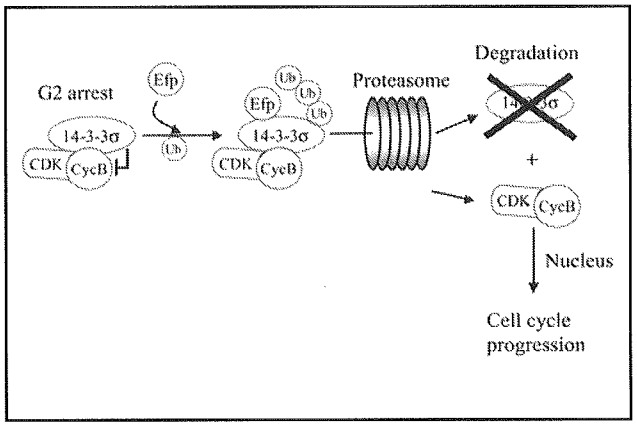

Figure 5. Models of Efp action as E3 ligase. Estrogen-induced RING finger protein Efp recognizes a cell cycle inhibitor 14-3-3Σ which keeps Cyclin B in cytoplasm. Efp modifies 14-3-3Σ with ubiquitin and the resulting ubiquitinated 14-3-3Σ is recruited to 26S proteosome to be destroyed. The dissociated cyclin B is now capable of entering the nucleus where it drives cell cycle.

MID1. It has been shown that MID1 associates with microtubules, whereas mutant forms of MID1 do not.[64] These results suggest that MIDI has a physiological role in microtubule dynamics.

Recently, the α4 protein, a regulatory subunit of protein phosphatase 2A (PP2A)[65] was isolated by yeast two-hybrid screening with MID1 as bait. It was demonstrated that the B-box 1 is sufficient for a strong interaction with α4. MID2,[66] which is highly similar to MID1, also binds α4. Cellular localizations of MID1 and α4 are coincident with cytoskeletal structures and MID1 with a mutation at the C terminus that mimics the mutant protein of some individuals with OS results in the formation of cytoplasmic clumps containing both proteins. The identified substrate for E3 ligase activity of MID1 is a cytosolic PP2A. In contrast, addition of a proteasome inhibitor to OS-derived fibroblasts expressing dysfunctional MID1 does not cause either enrichment of PP2A or accumulation of the enzyme's polyubiquitinated forms,[67] suggesting that MID1 mutations result in decreased proteolysis of the C subunit of PP2A in individuals with OS.

PML

PML also belongs to a subfamily of proteins containing a RBCC/TRIM motif.[43,68] PML has been implicated in the pathogenesis of acute promyelocytic leukemia that arises following a reciprocal chromosomal translocation that fuses the *PML* gene located on chromosome 15 with the retinoic acid receptor alpha (*RARα*) gene located on chromosome 17. The resulting PML-RARα fusion protein preserves most of the functional domains of both PML and RARα, but it lacks C-terminus of PML and N-terminus of RARα The fusion protein shows cell type- and promoter-specific differences from the wild type RARα,[25,26,69] while it maintains a responsiveness to retinoic acid. Overexpression of PML-RARα inhibits vitamin D3 and transforming growth factor β-induced differentiation and also reduces serum starvation-induced apoptosis in U937 cells.[70] In addition, dimerization of PML with PML-RARα is required to block differentiation.[71] Thus, PML-RARα is considered to function as a dominant negative protein by interfering with the function of PML and RARα.

In normal cells, cellular distribution of PML is found to form a discrete subnuclear compartment (nuclear body, NB)[72,73] or PML oncogenic domain.[74] Other proteins containing Sp100[75] and PLZF (for promyelocytic leukemia zinc finger)[76] have been reported to localize to the NBs. Interestingly, PLZF-RARα fusion protein is also found in a rare form of APL.[77] It is shown that the nuclear bodies were dispersed into a microspeckle pattern in APL cells but reformed with retinoic acid treatment by which APL cells differentiated into granulocytes. In addition, the NB is the preferred site where the early steps of transcription and replication of DNA virus occurs.[78] Therefore, the regulation of NB formation is thought to be involved in the pathogenesis of APL. Recently, PML is shown to be covalently modified by SUMO-1 (Small Ubiquitin-like Modifier-1) of ubiquitin-like proteins.[79] Mutations in the PML RING finger disrupt the nuclear body formation in vivo[3,69] and cause a failure of growth suppression,[80,81] apoptosis and anti-viral activities[82] of PML. The dependence on an intact RING finger for PML NBs formation implies specific protein interactions regulated by the RING structure. Recent studies have shown that PML RING interacting with the SUMO-1 E2 enzyme UBC9 is SUMO modified and the sumolylation of PML has an important role in regulating the formation of NBs.[83]

PML has two B-boxes (B1 and B2) adjacent to the RING domain. Mutations of conserved zinc-chelating residues in B1 and/or B2 boxes collapsed PML NB formation, whereas they did not affect PML oligomerization.[84] PML B-boxes are also involved in growth suppression.[80] It has been revealed that PML is sumoylated in B1 box which is responsible for binding of the 11S proteasomal subunit to PML NBs.[85]

The coiled coil region in PML is indispensable for multimerization or heterodimerization with PML-RARα,[69,71,86] formation of PML NB and growth suppression activity.[80] Notably, the important role of the coiled coil domain for the complex formation is also suggested from the studies of other RBCC/TRIM subfamily.[43,57]

TRIM8

TRIM8, a member of RBCC subfamily, is shown to interact with SOCS-1 (suppressor of cytokine signaling-1) which is induced by cytokines and inhibits cytokine signaling by binding to downstream signaling molecules such as JAK (Janus kinase) kinases.[87-89] The B-box coiled coil region of TRIM8 is sufficient for efficient interaction with SOCS-1, but the RING portion of the protein is not required for the binding. By contrast, both the SOCS box and the SH2 domain in SOCS-1 appear to be necessary for the interaction between SOCS-1 and TRIM8. It was found that exogenous coexpression of TRIM8/GERP with SOCS-1 decreased the stability of SOCS-1 protein and TRIM8 restored the IFN-γ-mediated transcription which was inhibited by the expression of SOCS-1.[90] These results suggest that TRIM8 is the putative E3 ligase for SOCS-1 and inhibits SOCS-1 function by targeting it for proteasomal degradation.

TRIM11

TRIM11 is a member of the protein family composed of a RING finger domain, which is a putative E3 ubiquitin ligase, a B-box domain, a coiled coil domain and a SPRY domain. A recent experiment with yeast two-hybrid screening has revealed that TRIM11 can interact with Humanin[91] which is a newly identified anti-apoptotic peptide that specifically suppresses Alzheimer's disease (AD)-related neurotoxicity. It is known that Bax

(Bcl2-associated X protein) has a crucial role in apoptosis. In response to death stimuli, Bax protein changes the conformation exposing membrane-targeting domains, translocates to mitochondrial membrane and releases the cytochrome c and other apoptogenic proteins. Indeed, Humanin is shown to bind with Bax and prevents the translocation of Bax from cytosol to mitochondria.[92] Moreover, Humanin blocks Bax association with isolated mitochondria and suppresses cytochrome c release. Therefore, Humanin seems to exert its anti-apoptotic effect by interfering the Bax function.

The coiled coil domain of TRIM11 is indispensable for the interaction with Humanin. The SPRY domain also contributes to the recognition of Humanin, whereas SPRY domain alone cannot. It was found that the intracellular level of Humanin was drastically reduced by the coexpression of TRIM11, and mutation of the RING finger domain or treatment with proteasome inhibitor attenuates the effect of TRIM11 on the intracellular level of Humanin.[91] These results suggest that the TRIM11 participates in the ubiquitin-mediated degradation of Humanin as an E3 ligase.

SSA/Ro (SSA1, TRIM21)

Sjögren syndrome is an autoimmune disease in which exocrine glands including salivary and lacrimal glands develop a chronic inflammation, and whose symptoms are dry eyes, dry mouth and fatigue. Autoantibodies to Ro recognize a ribonucleoprotein complex composed of small single-stranded RNAs and of one or more peptides. Although the Ro autoantigen is heterogeneous and found in most tissues and cells with differences in structure and quantity across tissues, it is detected in 35 to 50% of patients with systemic lupus erythematosus and in up to 97% of patients with Sjögren syndrome.[93] The 60-kD protein (Ro60) and the 52-kD protein (Ro52) were identified[94] and, another novel 56-kD protein (Ro56/SS-56) has been identified, recently.[95] Ro52 and Ro56 proteins belong to RBCC-SPRY subfamily. It is thought that the Ro autoantigen is involved in the regulation of transcription because it possesses functional domains associated with gene-regulation and binds to nucleic acids.[93] Its precise function is not understood, however. In a study, Ro52 was reported to be ubiquitinated in the cell.[96] The observation suggests that Ro52 may be downregulated by the ubiquitin–proteasome pathway in vivo. Interestingly, sera from patients with Sjögren syndrome showed heterogeneity in their reactivity to poly-ubiquitinated Ro52, probably because of their differing antigenic determinants. This heterogeneity of the reactivity may be associated with the varying clinical features found in Sjögren patients.

Conclusion

Here, we summarized the structural characteristics and functions of RING finger proteins specifically in terms of the E3 ligase activity. However, relatively few proteins have been really proven to function as E3 ligase. Thus, most RING finger proteins remain to be further investigated. Investigation of the RING finger proteins as a novel E3 ligase family will elucidate important mechanisms of cellular protein degradation and provide new insight into the physiological and pathophysiological roles of the pathway. Particularly, the molecular mechanisms of specific substrate recognition by E3 with the RING and other associated domains must be determined. Moreover, the RING finger proteins such as PML may possess unknown functions other than E3 ligase. Functional analysis of the RING finger proteins will help to understand biological roles of the family including the ubiquitin-mediated protein degradation pathway.

References

1. Freemont PS, Hanson IM, Trowsdale J. A novel cysteine-rich sequence motif. Cell 1991; 64(3):483-484.
2. Lovering R, Hanson IM, Borden KL et al. Identification and preliminary characterization of a protein motif related to the zinc finger. Proc Natl Acad Sci USA 1993; 90(6):2112-2116.
3. Borden KL, Boddy MN, Lally J et al. The solution structure of the RING finger domain from the acute promyelocytic leukaemia proto-oncoprotein PML. Embo J 1995; 14(7):1532-1541.
4. Barlow PN, Luisi B, Milner A et al. Structure of the C3HC4 domain by 1H-nuclear magnetic resonance spectroscopy. A new structural class of zinc-finger. J Mol Biol 1994; 237(2):201-211.
5. Bellon SF, Rodgers KK, Schatz DG et al. Crystal structure of the RAG1 dimerization domain reveals multiple zinc-binding motifs including a novel zinc binuclear cluster. Nat Struct Biol 1997; 4(7):586-591.
6. Gervais V, Busso D, Wasielewski E et al. Solution structure of the N-terminal domain of the human TFIIH MAT1 subunit: New insights into the RING finger family. J Biol Chem 2001; 276(10):7457-7464.
7. Zheng N, Wang P, Jeffrey PD et al. Structure of a c-Cbl-UbcH7 complex: RING domain function in ubiquitin-protein ligases. Cell 2000; 102(4):533-539.
8. Freemont PS. The RING finger. A novel protein sequence motif related to the zinc finger. Ann N Y Acad Sci 1993; 684:174-192.
9. Saurin AJ, Borden KL, Boddy MN et al. Does this have a familiar RING? Trends Biochem Sci 1996; 21(6):208-214.
10. Takeuchi M, Rothe M, Goeddel DV. Anatomy of TRAF2. Distinct domains for nuclear factor-kappaB activation and association with tumor necrosis factor signaling proteins. J Biol Chem 1996; 271(33):19935-19942.
11. Sato T, Irie S, Reed JC. A novel member of the TRAF family of putative signal transducing proteins binds to the cytosolic domain of CD40. FEBS Lett 1995; 358(2):113-118.
12. Cheng G, Cleary AM, Ye ZS et al. Involvement of CRAF1, a relative of TRAF, in CD40 signaling. Science 1995; 267(5203):1494-1498.
13. Rothe M, Sarma V, Dixit VM et al. TRAF2-mediated activation of NF-kappa B by TNF receptor 2 and CD40. Science 1995; 269(5229):1424-1427.
14. Takahashi R, Deveraux Q, Tamm I et al. A single BIR domain of XIAP sufficient for inhibiting caspases. J Biol Chem 1998; 273(14):7787-7790.
15. Liston P, Fong WG, Kelly NL et al. Identification of XAF1 as an antagonist of XIAP anti-Caspase activity. Nat Cell Biol 2001; 3(2):128-133.
16. Yang Y, Fang S, Jensen JP et al. Ubiquitin protein ligase activity of IAPs and their degradation in proteasomes in response to apoptotic stimuli. Science 2000; 288(5467):874-877.
17. Clem RJ, Miller LK. Control of programmed cell death by the baculovirus genes p35 and iap. Mol Cell Biol 1994; 14(8):5212-5222.
18. van der Reijden BA, Erpelinck-Verschueren CA, Lowenberg B et al. TRIADs: A new class of proteins with a novel cysteine-rich signature. Protein Sci 1999; 8(7):1557-1561.
19. Kitada T, Asakawa S, Hattori N et al. Mutations in the parkin gene cause autosomal recessive juvenile parkinsonism. Nature 1998; 392(6676):605-608.
20. Morett E, Bork P. A novel transactivation domain in parkin. Trends Biochem Sci 1999; 24(6):229-231.
21. Imai Y, Soda M, Inoue H et al. An unfolded putative transmembrane polypeptide, which can lead to endoplasmic reticulum stress, is a substrate of Parkin. Cell 2001; 105(7):891-902.
22. Imai Y, Soda M, Hatakeyama S et al. CHIP is associated with Parkin, a gene responsible for familial Parkinson's disease, and enhances its ubiquitin ligase activity. Mol Cell 2002; 10(1):55-67.

23. Zhang Y, Gao J, Chung KK et al. Parkin functions as an E2-dependent ubiquitin- protein ligase and promotes the degradation of the synaptic vesicle-associated protein, CDCrel-1. Proc Natl Acad Sci USA 2000; 97(24):13354-13359.
24. Reddy BA, Etkin LD, Freemont PS. A novel zinc finger coiled-coil domain in a family of nuclear proteins. Trends Biochem Sci 1992; 17(9):344-345.
25. Kakizuka A, Miller Jr WH, Umesono K et al. Chromosomal translocation t(15;17) in human acute promyelocytic leukemia fuses RAR alpha with a novel putative transcription factor, PML. Cell 1991; 66(4):663-674.
26. de The H, Lavau C, Marchio A et al. The PML-RAR alpha fusion mRNA generated by the t(15;17) translocation in acute promyelocytic leukemia encodes a functionally altered RAR. Cell 1991; 66(4):675-684.
27. Goddard AD, Borrow J, Freemont PS et al. Characterization of a zinc finger gene disrupted by the t(15;17) in acute promyelocytic leukemia. Science 1991; 254(5036):1371-1374.
28. Miki Y, Swensen J, Shattuck-Eidens D et al. A strong candidate for the breast and ovarian cancer susceptibility gene BRCA1. Science 1994; 266(5182):66-71.
29. Le Douarin B, Zechel C, Garnier JM et al. The N-terminal part of TIF1, a putative mediator of the ligand-dependent activation function (AF-2) of nuclear receptors, is fused to B-raf in the oncogenic protein T18. Embo J 1995; 14(9):2020-2033.
30. Hershko A, Ciechanover A. The ubiquitin system. Annu Rev Biochem 1998; 67:425-479.
31. Joazeiro CA, Wing SS, Huang H et al. The tyrosine kinase negative regulator c-Cbl as a RING-type, E2-dependent ubiquitin-protein ligase. Science 1999; 286(5438):309-312.
32. Lorick KL, Jensen JP, Fang S et al. RING fingers mediate ubiquitin-conjugating enzyme (E2)-dependent ubiquitination. Proc Natl Acad Sci USA 1999; 96(20):11364-11369.
33. Urano T, Saito T, Tsukui T et al. Efp targets 14-3-3 sigma for proteolysis and promotes breast tumour growth. Nature 2002; 417(6891):871-875.
34. Zhang Y, Xiong Y. Control of p53 ubiquitination and nuclear export by MDM2 and ARF. Cell Growth Differ 2001; 12(4):175-186.
35. Seol JH, Feldman RM, Zachariae W et al. Cdc53/cullin and the essential Hrt1 RING-H2 subunit of SCF define a ubiquitin ligase module that activates the E2 enzyme Cdc34. Genes Dev 1999; 13(12):1614-1626.
36. Galisteo ML, Dikic I, Batzer AG et al. Tyrosine phosphorylation of the c-cbl proto-oncogene protein product and association with epidermal growth factor (EGF) receptor upon EGF stimulation. J Biol Chem 1995; 270(35):20242-20245.
37. Thien CB, Walker F, Langdon WY. RING finger mutations that abolish c-Cbl-directed polyubiquitination and downregulation of the EGF receptor are insufficient for cell transformation. Mol Cell 2001; 7(2):355-365.
38. Haupt Y, Maya R, Kazaz A et al. Mdm2 promotes the rapid degradation of p53. Nature 1997; 387(6630):296-299.
39. Kubbutat MH, Jones SN, Vousden KH. Regulation of p53 stability by Mdm2. Nature 1997; 387(6630):299-303.
40. Geyer RK, Yu ZK, Maki CG. The MDM2 RING-finger domain is required to promote p53 nuclear export. Nat Cell Biol 2000; 2(9):569-573.
41. Chen Y, Chen CF, Riley DJ et al. Aberrant subcellular localization of BRCA1 in breast cancer. Science 1995; 270(5237):789-791.
42. Lupas A. Coiled coils: New structures and new functions. Trends Biochem Sci 1996; 21(10):375-382.
43. Reymond A, Meroni G, Fantozzi A et al. The tripartite motif family identifies cell compartments. Embo J 2001; 20(9):2140-2151.
44. Tissot C, Mechti N. Molecular cloning of a new interferon-induced factor that represses human immunodeficiency virus type 1 long terminal repeat expression. J Biol Chem 1995; 270(25):14891-14898.
45. Der SD, Zhou A, Williams BR et al. Identification of genes differentially regulated by interferon alpha, beta, or gamma using oligonucleotide arrays. Proc Natl Acad Sci USA 1998; 95(26):15623-15628.
46. Orimo A, Tominaga N, Yoshimura K et al. Molecular cloning of ring finger protein 21 (RNF21)/interferon-responsive finger protein (ifp1), which possesses two RING-B box-coiled coil domains in tandem. Genomics 2000; 69(1):143-149.
47. Slack FJ, Ruvkun G. A novel repeat domain that is often associated with RING finger and B-box motifs. Trends Biochem Sci 1998; 23(12):474-475.
48. Lu Z, Xu S, Joazeiro C et al. The PHD domain of MEKK1 acts as an E3 ubiquitin ligase and mediates ubiquitination and degradation of ERK1/2. Mol Cell 2002; 9(5):945-956.
49. Dhalluin C, Carlson JE, Zeng L et al. Structure and ligand of a histone acetyltransferase bromodomain. Nature 1999; 399(6735):491-496.
50. Ancient missense mutations in a new member of the RoRet gene family are likely to cause familial Mediterranean fever. The International FMF Consortium. Cell 1997; 90(4):797-807.
51. Quaderi NA, Schweiger S, Gaudenz K et al. Opitz G/BBB syndrome, a defect of midline development, is due to mutations in a new RING finger gene on Xp22. Nat Genet 1997; 17(3):285-291.
52. Avela K, Lipsanen-Nyman M, Idanheimo N et al. Gene encoding a new RING-B-box-Coiled-coil protein is mutated in mulibrey nanism. Nat Genet 2000; 25(3):298-301.
53. Cao T, Borden KL, Freemont PS et al. Involvement of the rfp tripartite motif in protein-protein interactions and subcellular distribution. J Cell Sci 1997; 110(Pt 14):1563-1571.
54. Shimono Y, Murakami H, Hasegawa Y et al. RET finger protein is a transcriptional repressor and interacts with enhancer of polycomb that has dual transcriptional functions. J Biol Chem 2000; 275(50):39411-39419.
55. Cao T, Duprez E, Borden KL et al. Ret finger protein is a normal component of PML nuclear bodies and interacts directly with PML. J Cell Sci 1998; 111(Pt 10):1319-1329.
56. Trockenbacher A, Suckow V, Foerster J et al. MID1, mutated in Opitz syndrome, encodes an ubiquitin ligase that targets phosphatase 2A for degradation. Nat Genet 2001; 29(3):287-294.
57. Peng H, Begg GE, Schultz DC et al. Reconstitution of the KRAB-KAP-1 repressor complex: A model system for defining the molecular anatomy of RING-B box-coiled-coil domain-mediated protein-protein interactions. J Mol Biol 2000; 295(5):1139-1162.
58. Inoue S, Orimo A, Hosoi T et al. Genomic binding-site cloning reveals an estrogen-responsive gene that encodes a RING finger protein. Proc Natl Acad Sci USA 1993; 90(23):11117-11121.
59. Orimo A, Inoue S, Ikeda K et al. Molecular cloning, structure, and expression of mouse estrogen-responsive finger protein Efp. Colocalization with estrogen receptor mRNA in target organs. J Biol Chem 1995; 270(41):24406-24413.
60. Ikeda K, Orimo A, Higashi Y et al. Efp as a primary estrogen-responsive gene in human breast cancer. FEBS Lett 2000; 472(1):9-13.
61. Orimo A, Inoue S, Minowa O et al. Underdeveloped uterus and reduced estrogen responsiveness in mice with disruption of the estrogen-responsive finger protein gene, which is a direct target of estrogen receptor alpha. Proc Natl Acad Sci USA 1999; 96(21):12027-12032.
62. Opitz JM. G syndrome (hypertelorism with esophageal abnormality and hypospadias, or hypospadias-dysphagia, or "Opitz-Frias" or "Opitz-G" syndrome)—perspective in 1987 and bibliography. Am J Med Genet 1987; 28(2):275-285.
63. Robin NH, Opitz JM, Muenke M. Opitz G/BBB syndrome: Clinical comparisons of families linked to Xp22 and 22q, and a review of the literature. Am J Med Genet 1996; 62(3):305-317.
64. Gaudenz K, Roessler E, Quaderi N et al. Opitz G/BBB syndrome in Xp22: Mutations in the MID1 gene cluster in the carboxy-terminal domain. Am J Hum Genet 1998; 63(3):703-710.
65. Jerome LA, Papaioannou VE. DiGeorge syndrome phenotype in mice mutant for the T-box gene, Tbx1. Nat Genet 2001; 27(3):286-291.
66. Cainarca S, Messali S, Ballabio A et al. Functional characterization of the Opitz syndrome gene product (midin): Evidence for homodimerization and association with microtubules throughout the cell cycle. Hum Mol Genet 1999; 8(8):1387-1396.

67. Short KM, Hopwood B, Yi Z et al. MID1 and MID2 homo- and heterodimerise to tether the rapamycin-sensitive PP2A regulatory subunit, alpha 4, to microtubules: Implications for the clinical variability of X-linked Opitz GBBB syndrome and other developmental disorders. BMC Cell Biol 2002; 3(1):1.
68. Borden KL. RING fingers and B-boxes: Zinc-binding protein-protein interaction domains. Biochem Cell Biol 1998; 76(2-3):351-358.
69. Kastner P, Perez A, Lutz Y et al. Structure, localization and transcriptional properties of two classes of retinoic acid receptor alpha fusion proteins in acute promyelocytic leukemia (APL): Structural similarities with a new family of oncoproteins. Embo J 1992; 11(2):629-642.
70. Grignani F, Ferrucci PF, Testa U et al. The acute promyelocytic leukemia-specific PML-RAR alpha fusion protein inhibits differentiation and promotes survival of myeloid precursor cells. Cell 1993; 74(3):423-431.
71. Grignani F, Testa U, Rogaia D et al. Effects on differentiation by the promyelocytic leukemia PML/RARalpha protein depend on the fusion of the PML protein dimerization and RARalpha DNA binding domains. Embo J 1996; 15(18):4949-4958.
72. Weis K, Rambaud S, Lavau C et al. Retinoic acid regulates aberrant nuclear localization of PML-RAR alpha in acute promyelocytic leukemia cells. Cell 1994; 76(2):345-356.
73. Koken MH, Puvion-Dutilleul F, Guillemin MC et al. The t(15;17) translocation alters a nuclear body in a retinoic acid-reversible fashion. Embo J 1994; 13(5):1073-1083.
74. Dyck JA, Maul GG, Miller Jr WH et al. A novel macromolecular structure is a target of the promyelocyte-retinoic acid receptor oncoprotein. Cell 1994; 76(2):333-343.
75. Szostecki C, Guldner HH, Netter HJ et al. Isolation and characterization of cDNA encoding a human nuclear antigen predominantly recognized by autoantibodies from patients with primary biliary cirrhosis. J Immunol 1990; 145(12):4338-4347.
76. Koken MH, Reid A, Quignon F et al. Leukemia-associated retinoic acid receptor alpha fusion partners, PML and PLZF, heterodimerize and colocalize to nuclear bodies. Proc Natl Acad Sci USA 1997; 94(19):10255-10260.
77. Chen Z, Brand NJ, Chen A et al. Fusion between a novel Kruppel-like zinc finger gene and the retinoic acid receptor-alpha locus due to a variant t(11;17) translocation associated with acute promyelocytic leukaemia. Embo J 1993; 12(3):1161-1167.
78. Ishov AM, Maul GG. The periphery of nuclear domain 10 (ND10) as site of DNA virus deposition. J Cell Biol 1996; 134(4):815-826.
79. Kamitani T, Nguyen HP, Kito K et al. Covalent modification of PML by the sentrin family of ubiquitin-like proteins. J Biol Chem 1998; 273(6):3117-3120.
80. Fagioli M, Alcalay M, Tomassoni L et al. Cooperation between the RING + B1-B2 and coiled-coil domains of PML is necessary for its effects on cell survival. Oncogene 1998; 16(22):2905-2913.
81. Mu ZM, Chin KV, Liu JH et al. PML, a growth suppressor disrupted in acute promyelocytic leukemia. Mol Cell Biol 1994; 14(10):6858-6867.
82. Regad T, Saib A, Lallemand-Breitenbach V et al. PML mediates the interferon-induced antiviral state against a complex retrovirus via its association with the viral transactivator. Embo J 2001; 20(13):3495-3505.
83. Kamitani T, Kito K, Nguyen HP et al. Identification of three major sentrinization sites in PML. J Biol Chem 1998; 273(41):26675-26682.
84. Borden KL, Lally JM, Martin SR et al. In vivo and in vitro characterization of the B1 and B2 zinc-binding domains from the acute promyelocytic leukemia protooncoprotein PML. Proc Natl Acad Sci USA 1996; 93(4):1601-1606.
85. Lallemand-Breitenbach V, Zhu J, Puvion F et al. Role of promyelocytic leukemia (PML) sumolation in nuclear body formation, 11S proteasome recruitment, and As2O3-induced PML or PML/retinoic acid receptor alpha degradation. J Exp Med 2001; 193(12):1361-1371.
86. Le XF, Yang P, Chang KS. Analysis of the growth and transformation suppressor domains of promyelocytic leukemia gene, PML. J Biol Chem 1996; 271(1):130-135.
87. Chen XP, Losman JA, Rothman P. SOCS proteins, regulators of intracellular signaling. Immunity 2000; 13(3):287-290.
88. Haque SJ, Harbor PC, Williams BR. Identification of critical residues required for suppressor of cytokine signaling-specific regulation of interleukin-4 signaling. J Biol Chem 2000; 275(34):26500-26506.
89. Terstegen L, Maassen BG, Radtke S et al. Differential inhibition of IL-6-type cytokine-induced STAT activation by PMA. FEBS Lett 2000; 478(1-2):100-104.
90. Toniato E, Chen XP, Losman J et al. TRIM8/GERP RING finger protein interacts with SOCS-1. J Biol Chem 2002; 277(40):37315-37322.
91. Niikura T, Hashimoto Y, Tajima H et al. A tripartite motif protein TRIM11 binds and destabilizes Humanin, a neuroprotective peptide against Alzheimer's disease-relevant insults. Eur J Neurosci 2003; 17(6):1150-1158.
92. Guo B, Zhai D, Cabezas E et al. Humanin peptide suppresses apoptosis by interfering with Bax activation. Nature 2003; 423(6938):456-461.
93. Sibilia J. Ro(SS-A) and anti-Ro(SS-A): An update. Rev Rhum Engl Ed 1998; 65(1):45-57.
94. Itoh Y, Reichlin M. Autoantibodies to the Ro/SSA antigen are conformation dependent. I: Anti-60 kD antibodies are mainly directed to the native protein; anti-52 kD antibodies are mainly directed to the denatured protein. Autoimmunity 1992; 14(1):57-65.
95. Billaut-Mulot O, Cocude C, Kolesnitchenko V et al. SS-56, a novel cellular target of autoantibody responses in Sjogren syndrome and systemic lupus erythematosus. J Clin Invest 2001; 108(6):861-869.
96. Fukuda-Kamitani T, Kamitani T. Ubiquitination of Ro52 autoantigen. Biochem Biophys Res Commun 2002; 295(4):774-778.

Oncogene (2005) 24, 4754–4764

www.nature.com/onc

Tyrosine phosphorylation of paxillin affects the metastatic potential of human osteosarcoma

Kotaro Azuma[1,2], Masamitsu Tanaka[1], Takamasa Uekita[1], Satoshi Inoue[2], Jun Yokota[3], Yasuyoshi Ouchi[2] and Ryuichi Sakai*[,1]

[1]*Growth Factor Division, National Cancer Center Research Institute, 5-1-1 Tsukiji, Chuo-ku, Tokyo 104-0045, Japan;* [2]*Department of Geriatric Medicine, Graduate School of Medicine, The University of Tokyo, 7-3-1, Hongo, Bunkyo-ku, 113-8655, Tokyo, Japan;* [3]*Division of Biology, National Cancer Center Research Institute, 5-1-1 Tsukiji, Chuo-ku, Tokyo 104-0045, Japan*

To acquire information on signal alteration corresponding to the changes in metastatic potential, we analysed protein tyrosine phosphorylation of low- and high-metastatic human osteosarcoma HuO9 sublines, which were recently established as the first metastatic model of human osteosarcoma. Tyrosine phosphorylation of proteins around 60, 70, and 120–130 kDa was enhanced in high-metastatic sublines. Among these proteins, the protein around 70 kDa, which was most remarkably phosphorylated, was identified as paxillin, a scaffold protein in integrin signaling. Activity of Src family kinase correlated well with metastatic potential, and a Src family kinase inhibitor, PP2, not only abolished tyrosine phosphorylation of paxillin but also impaired the motility of high-metastatic sublines. The expression of paxillin was also elevated in high-metastatic sublines, and knocking down of paxillin expression by RNAi method resulted in attenuated motility of high-metastatic cells. We also demonstrated that the phosphorylated form of paxillin is essential for the migration-promoting effect in human osteosarcoma. These findings suggest that enhanced activity of Src family kinases and overexpression of paxillin synergistically contribute to the high metastatic potential of human osteosarcoma through the hyperphosphorylation of paxillin.
Oncogene (2005) **24,** 4754–4764. doi:10.1038/sj.onc.1208654; published online 2 May 2005

Keywords: osteosarcoma; pulmonary metastasis; paxillin; tyrosine phosphorylation; Src family kinase; motility

Introduction

Multiple steps of tumor metastasis are regulated by various external stimuli such as hormones, cytokines and extracellular matrices. As major mediators of these stimuli, both receptor and nonreceptor tyrosine kinases play important roles to elicit intracellular signal transduction in response to the metastatic environment of tumor cells (Pawson, 2004). Various processes such as cell adhesion, anchorage-independent growth, cell motility, and cell invasion, which are essential components of tumor metastasis, are regulated by tyrosine phosphorylation. Indeed, the activation of Src family tyrosine kinases is frequently found during proliferation and metastasis of human cancers (Yeatman, 2004), indicating that tumor progression is reflected by the activity of tyrosine kinase and phosphorylation states of substrates in metastatic tumors.

Osteosarcoma is a primary malignant bone tumor that usually affects teenagers and frequent metastasis to the lungs is a clinical characteristic of osteosarcoma. As many as 20% of patients are estimated to have pulmonary metastases at the time of diagnosis and their prognosis is extremely poor with 10–20% 5-year survival rate (Meyers *et al.*, 1993; Tsuchiya *et al.*, 2002). Even though patients did not have metastases at the time of diagnosis, 35–50% of them developed pulmonary metastases during treatment (Huth and Eilber, 1989; Ward *et al.*, 1994). For this reason, pulmonary metastasis of osteosarcoma requires effective prevention and treatment.

Investigation of pulmonary metastasis of human osteosarcoma was impeded by the lack of a proper metastatic model of human osteosarcoma cell lines. Recently, Kimura *et al.* (2002) established human osteosarcoma cell lines with high metastatic potential to the lungs for the first time. From parental HuO9 cells, M112 and M132 were established as high-metastatic sublines, which developed more than 200 macroscopic metastatic nodules in the lungs after injection of 2×10^6 cells into the tail vein of nude mice. On the other hand, L12 and L13 are low-metastatic sublines established by the dilution plating method from the same parent HuO9 cells (Nakano *et al.*, 2003). These sublines developed only 0–15 macroscopic nodules in the lungs after injection of 2×10^6 cells and all mice survived up to 200 days.

In order to acquire information on signal alteration corresponding to the changes in metastatic potential, we compared the profile of protein tyrosine phosphorylation by utilizing these HuO9-derived sublines. A 68 kDa cytoskeletal protein, paxillin, was identified as

*Correspondence: R Sakai; E-mail: rsakai@gan2.res.ncc.go.jp
Received 8 October 2004; revised 21 January 2005; accepted 25 February 2005; published online 2 May 2005

a molecule that shows the most outstanding difference in phosphorylation state between low- and high-metastatic sublines among several phosphotyrosine-containing proteins that are differentially phosphorylated in these sublines. Paxillin has no intrinsic enzymatic activity, but it has multiple domains that interact with cytoskeletal and signaling molecules, and functions as a scaffold protein at focal adhesions (Turner, 2000; Schaller, 2001). Paxillin contains two critical tyrosine phosphorylation sites at Tyr 31 and Tyr 118 (Schaller and Parsons, 1995). These phosphotyrosines are considered to serve as docking sites for other signaling molecules, but it remains controversial whether these phosphotyrosines have promoting effect or inhibitory effect on cell motility.

In this study, we show overexpression and hyperphosphorylation of paxillin in high-metastatic sublines of human osteosarcoma, indicating that, in the case of human osteosarcoma, tyrosine phosphorylation of paxillin has a promoting effect for cell migration. We also demonstrate that elevated activity of Src family kinases in high-metastatic sublines is essential for the enhanced motility for these osteosarcoma cells, suggesting the contribution of Src family kinase activity to the high metastatic potential of human osteosarcoma.

Results

General enhancement of tyrosine phosphorylation in high-metastatic HuO9 sublines

First, we confirmed the difference in motility between low- and high-metastatic sublines using Cell Culture Insert. High-metastatic sublines, M112 and M132, showed more than six times as high motility as low-metastatic sublines, L12 and L13 (data not shown). This result indicates that the motility of HuO9 sublines indeed correlates with their metastatic potential as previously reported (Nakano *et al.*, 2003).

To clarify the factors that determine the metastatic potential of HuO9 sublines, we compared expression patterns of phosphotyrosine-containing proteins between low- and high-metastatic sublines (Figure 1). General enhancement of tyrosine phosphorylation was observed in high-metastatic sublines, M112 and M132, as well as parental HuO9, which also has rather high metastatic potential (Nakano *et al.*, 2003). Among several phosphotyrosine-containing proteins showing elevated phosphorylation in high-metastatic sublines, the most striking difference was a broad band around 70 kDa (marked b in Figure 1). In addition, there were several other minor phosphotyrosine-containing proteins differentially expressed between low- and high-metastatic sublines, such as proteins around 60 kDa (marked c in Figure 1) and 120–130 kDa (marked a in Figure 1). These differences in tyrosine phosphorylation were consistent at different time points after plating (6 and 24 h) with and without fibronectin coating (Supplementary Figure 1 and data not shown).

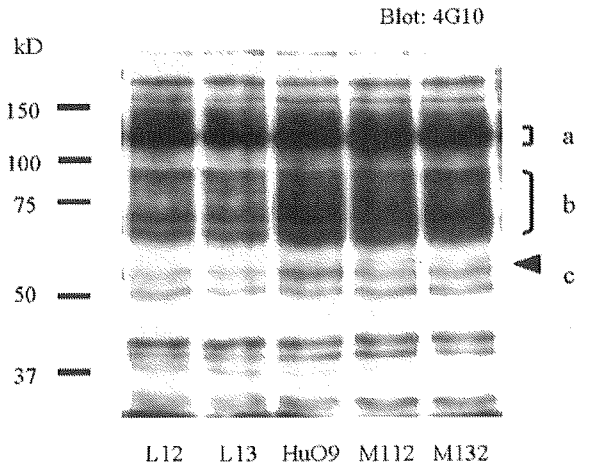

Figure 1 Elevated tyrosine phosphorylation of several proteins in high-metastatic sublines of HuO9 cells. Low-metastatic sublines (L12, L13), high-metastatic sublines (M112, M132) and parental HuO9 cells plated on plastic culture dishes for longer than 48 h were lysed for immunoblotting with anti-phosphotyrosine antibody 4G10. Hyperphosphorylated proteins in high-metastatic sublines are indicated on the right (a, b, c)

As candidate proteins of the difference around 120–130 kDa tyrosine phosphorylation, p130^{Cas} and focal adhesion kinase (FAK) were examined using phospho-specific antibodies (Figure 2). p130^{Cas} is a docking protein involved in the integrin signaling. We generated phospho-specific antibodies against several putative phosphorylation sites of p130^{Cas} and used them for the analysis. As a result, elevated phosphorylation of Tyr 762 was found in high-metastatic sublines (2.5 times as much as low-metastatic sublines), while phosphorylation of Tyr 460 of p130^{Cas} did not show obvious correlation with metastatic potential (Figure 2a). Tyr 460 represents tandem YDXP motifs in the substrate domain of p130^{Cas}, which binds (Crk) (Sakai *et al.*, 1994) or Nck (Schlaepfer *et al.*, 1997), and Tyr 762 consists of YDYV motif, which serves as a Src-binding site when phosphorylated (Nakamoto *et al.*, 1996). Expression of p130^{Cas} did not vary significantly among each subline (Figure 2a).

FAK is a nonreceptor tyrosine kinase, which is also involved in the integrin signaling, and its Tyr 397 is autophosphorylated when FAK is activated (Schaller *et al.*, 1994). The expression of FAK and phosphorylation on Tyr 397 of FAK were analysed. However, no remarkable elevation of tyrosine-phosphorylated FAK was detected in high-metastatic sublines (Figure 2b).

To identify the phosphotyrosine-containing protein around 60 kDa, the expression level and tyrosine phosphorylation of Src family kinases was examined. Among the members of Src family kinases, only Fyn kinase had the tendency of hyperphosphorylation in high-metastatic sublines (Figure 2c). Tyrosine phosphorylation of c-Src, Yes, and Fgr, other members of Src family kinases that were examined, did not correlate

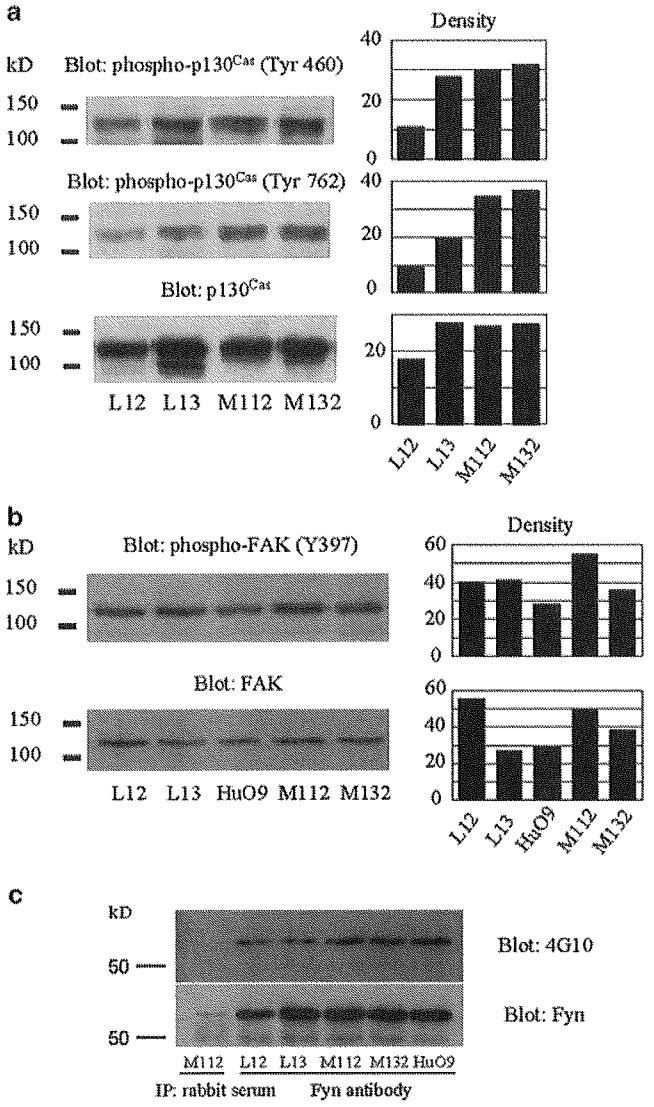

Figure 2 Elevated tyrosine phosphorylation of p130^{Cas} (Tyr 762) in high-metastatic sublines. (**a**) Whole-cell lysates from low-metastatic (L12, L13) and high-metastatic sublines (M112, M132) were immunoblotted for two kinds of anti-phosho-p130^{Cas} antibody (Tyr 460 representing the tandem YDXP motif, and Tyr 762 representing the YDYV motif in Src-binding domain) and p130^{Cas} antibody. Density of each blot was measured as described in Materials and methods. (**b**) Whole-cell lysates from low-metastatic (L12, L13), high-metastatic (M112, M132) and parental HuO9 were immunoblotted for anti-phospho-FAK antibody (Tyr 397) and anti-FAK antibody. Density of each blot was measured as described in Materials and methods. (**c**) Fyn kinase of low- and high-metastatic sublines was immunoprecipitated by anti-Fyn polyclonal antibody and subsequently immunoblotted with anti-phosphotyrosine antibody 4G10 or anti-Fyn antibody

with the metastatic potential (data not shown). However, absorption of Fyn by anti-Fyn antibody from lysates of low- and high-metastatic sublines could not remove the difference in tyrosine phosphorylation around 60 kDa (data not shown), indicating that not only Fyn contributes to the elevation of tyrosine phosphorylation around 60 kDa.

Overexpression and hyperphosphorylation of paxillin in high-metastatic HuO9 sublines

From the molecular size and the broad appearance of the 70 kDa protein, we estimated that this highly phosphorylated protein in high-metastatic sublines was paxillin. Using a specific antibody of phospho-paxillin (Tyr 118) for the blotting of whole-cell lysates, it was confirmed that high-metastatic sublines indeed contained a higher amount of tyrosine-phosphorylated paxillin in high-metastatic sublines (Figure 3A). It was also found that total paxillin expression was elevated in high-metastatic sublines compared with low-metastatic sublines (Figure 3A). As for both total paxillin and phospho-paxillin, high-metastatic sublines were estimated to contain about three to five times as much as low-metastatic sublines using densitometric analysis.

Absorption of paxillin by anti-paxillin antibody from lysates of low- and high-metastatic sublines remove most of the difference in tyrosine phosphorylation around 70 kDa (Figure 3B), indicating that paxillin mainly contributes to the elevation of tyrosine phosphorylation around 70 kDa.

Immunostaining of paxillin revealed that total paxillin and phospho-paxillin (Tyr 118) localize at focal adhesions, which were characterized at both ends of the actin filaments in L12 and M132 cells (Figure 3C). There was no significant change in the localization of paxillin by the metastatic potential of sublines, although the staining of total paxillin and phospho-paxillin were stronger in high-metastatic sublines than those in low-metastatic sublines (Figure 3D).

Src family kinase activity is elevated in the high-metastatic sublines

The general enhancement of tyrosine phosphorylation in high-metastatic sublines (Figure 1) suggests that the activity of some tyrosine kinases were enhanced in high-metastatic sublines. Therefore, we examined which tyrosine kinase is responsible for the high metastatic potential.

First, the difference in Src family kinase activity was investigated using Src-2 antibody, which is known to recognize wide ranges of Src family kinases. As a result, the activity of Src family kinases was elevated in the high-metastatic sublines compared with low-metastatic sublines (Figure 4a). The candidate for the Src family kinase responsible for the elevated kinase activity in high-metastatic sublines might be Fyn, which showed enhanced autophosphorylation in high-metastatic sublines (Figure 2c). We also examined the kinase activity of FAK and c-Abl, which are also reported to phosphorylate the tyrosine residues of paxillin. However, we observed a lack of correlation between kinase activity of FAK or c-Abl and metastatic potential (Figure 4b).

To check the influence of Src family kinase activity on cell motility elevated in high-metastatic sublines, cell migration assay was performed. In the high-metastatic sublines treated with PP2, an inhibitor of Src family kinases, motility was significantly suppressed, while in

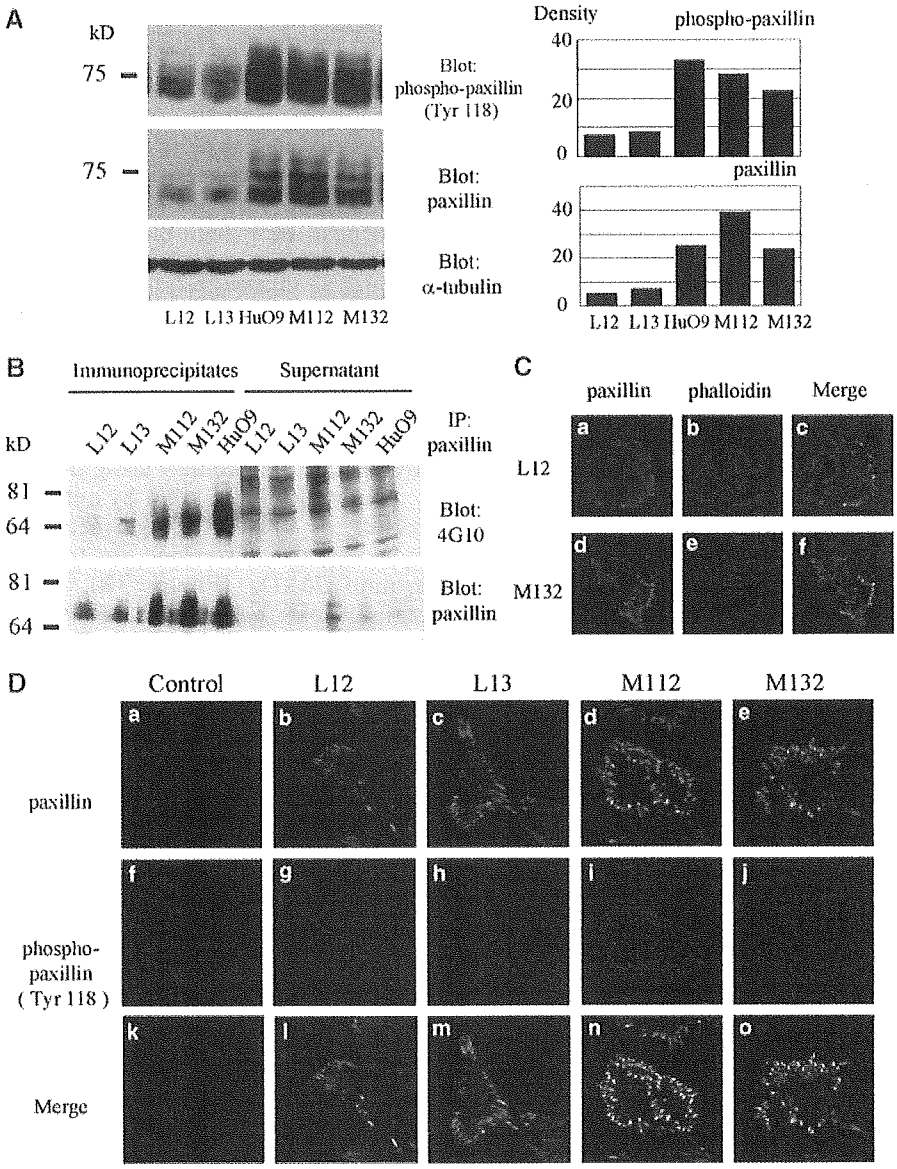

Figure 3 Overexpression and hyperphosphorylation of paxillin in high-metastatic sublines. (**A**) Whole-cell lysates from low-metastatic (L12, L13), high-metastatic (M112, M132) and parental HuO9 were immunoblotted for anti-phospho-paxillin antibody (Tyr 118), paxillin antibody and anti-α-tubulin antibody as an internal control. Densities of paxillin and phospho-paxillin blots are shown on the right. (**B**) Whole-cell lysates of low- and high-metastatic sublines and parental HuO9 cells were immunoprecipitated by monoclonal anti-paxillin antibody. Both immunoprecipitates and supernatants (indicated at the top) were subjected to immunoblotting analysis by anti-phosphotyrosine antibody 4G10 and anti-paxillin antibody. (**C**) L12 and M132 sublines were immunostained with anti-paxillin antibody (a, d: green), and chemically stained with phalloidin (b, e: red) at the same time. (**D**) Low- and high-metastatic sublines were immunostained with the antibody against paxillin (b–e: green) or phospho-paxillin (g–j: red). Superimposed confocal images (l–o: merge) demonstrate the portion of phosphorylated paxillin over the total paxillin. Images without first antibodies (a and f) are shown as negative controls. For comparison, panels were captured with identical gain and iris value and processed in the same way

the cells treated with PP3, inactive structural analog of PP2, their motility was not affected (Figure 4c). The effect of Src family kinase on the tyrosine phosphorylation of paxillin was also evaluated. When, high-metastatic sublines were treated with PP2, the tyrosine phosphorylation of paxillin was almost completely abolished, while the phosphorylation remained unchanged when the cells were treated with PP3 (Figure 4d). These results indicate that, in high-metastatic sublines of HuO9, tyrosine phosphorylation of paxillin and enhanced cell motility are mostly dependent on the activity of Src family kinases.

Cell migration was attenuated by knocking down of paxillin expression in high-metastatic sublines

To evaluate the direct involvement of paxillin in the cell motility of the osteosarcoma cells, paxillin expression was knocked down using RNA interference (RNAi) in high-metastatic HuO9 sublines. Using a novel approach

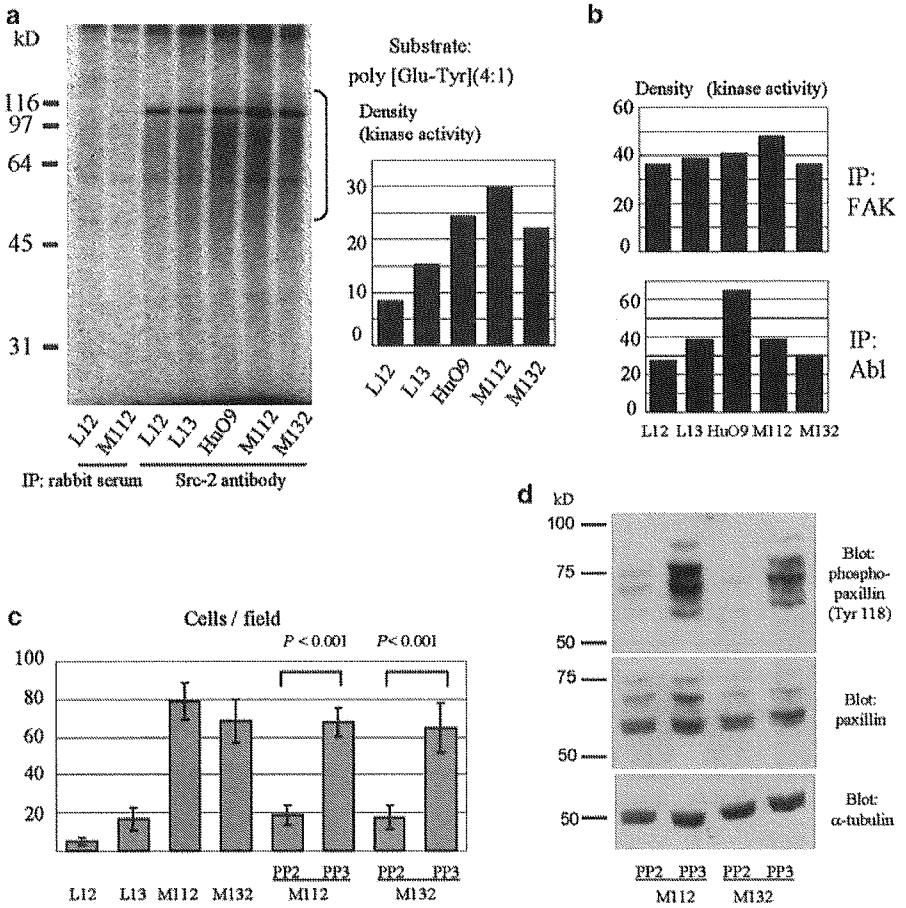

Figure 4 Elevated Src family kinase activity in high-metastatic sublines. (**a**) Elevated Src family kinase activity in high-metastatic sublines. Src family kinases of low- and high-metastatic sublines and parental HuO9 cell lysates were immunoprecipitated by Src-2 antibody. Lysates of L12 and M112 immunoprecipitated with preimmune rabbit serum were used as negative controls. Kinase activity was evaluated by phosphorylation of exogenous synthetic polypeptide poly[Glu-Tyr](4:1). The density of each smear (between 50 and 150 kDa, area shown by a bracket) was quantified. (**b**) FAK or c-Abl of low- and high-metastatic sublines and parental HuO9 were immunoprecipitated by monoclonal antibodies. To evaluate kinase activity, exogenous synthetic polypeptide poly[Glu-Tyr](4:1) was used. The kinase activities were quantified according to the same method as described in (**a**). (**c**) Src family kinase inhibitor PP2 (4-amino-5-(4-chlorophenyl)-7-(t-butyl)pyrazolo[3,4-d]pyrimidine) impairs the motility of high-metastatic sublines. Motility of low- and high-metastatic sublines and parental HuO9 cells was evaluated by migration assay as described in Materials and methods. As for high-metastatic sublines, M112 and M132, motility in the presence of 10 μM of PP2 or 10 μM of PP3 (4-amino-7-phenylpyrazol [3,4-d]pyrimidine) was also evaluated. The cells at the lower side of the filters were stained by Giemsa's stain solution and visualized under microscope at a magnification of $\times$ 200. Each bar represents the mean number of cells $\pm$ s.d. counted in five fields. (**d**) Src family kinase inhibitor PP2 abolishes tyrosine phosphorylation of paxillin. High-metastatic subline M112 and M132 were treated with 10 μM of PP2 or PP3 for 30 min prior to cell lysis. Whole-cell lysates were immunoblotted for anti-phospho-paxillin antibody, anti-paxillin antibody and anti-α-tubulin antibody

called the Dicer method to introduce a series of short interfering RNA (siRNA) into the cells, paxillin expression was suppressed by about 60%, while phospho-paxillin decreased by about 30% compared with LacZ siRNA-treated cells (Figure 5a).

Although the expression of paxillin was not completely suppressed, cell motility was impaired by about two-thirds by treatment with paxillin siRNA when compared with LacZ siRNA-treated cells (Figure 5b). This difference is statistically significant over nonspecific effects of siRNA on cell survival and motility.

This attenuation of motility was not observed when the expression of $p130^{Cas}$ was knocked down using the Dicer method in high-metastatic sublines (Supplementary Figure 2a, b). These results indicate paxillin rather than $p130^{Cas}$ is more closely associated with the motility of osteosarcoma sublines.

Overexpression of paxillin and elevation of Src family kinase activity synergistically enhance the motility of human osteosarcoma

To further examine the role of paxillin and its tyrosine phosphorylation on the motility of osteosarcoma sublines, the effect of transient transfection of GFP-paxillin and its phenylalanine mutant of two tyrosines (2F mutant) was evaluated. In 2F mutant, two critical tyrosine phosphorylation sites at Tyr 31 and Tyr 118

were mutated to phenylalanine, and these tyrosine residues were confirmed to be major phosphorylation sites by transient transfection of GFP-paxillin and GFP-2F mutant to COS-7 cells (Figure 6A).

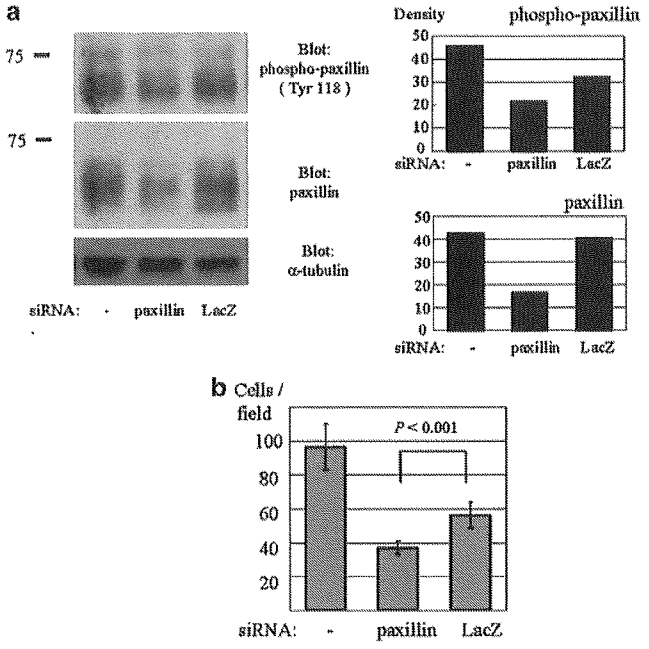

Figure 5 Cell migration was attenuated by knocking down of paxillin expression in high-metastatic sublines. (**a**) M112 subline was transfected with siRNA of paxillin or LacZ, or treated only with lipofection reagent ((−), as indicated at the bottom). Cells were lysed at 72 h from the transfection and whole-cell lysates were immunoblotted with the antibodies indicated. The density of each band is shown on the right. (**b**) M112 subline was transfected with siRNA or treated only with lipofection reagent as described above. Transfected cells were subjected to migration assay as described in Materials and methods

Next, GFP-paxillin and GFP-2F mutant were transiently expressed in the low-metastatic subline, L12 (Figure 6B, arrowhead in lower panel). The tyrosine phosphorylation of GFP-paxillin was detected by phospho-paxillin (Tyr 118) antibody in L12 (Figure 6B, arrowhead in upper panel), although this polyclonal antibody showed slight reactivity even to the 2F mutant of paxillin. Both GFP-paxillin and GFP-2F mutant were confirmed to localize at focal adhesions (Figure 6C).

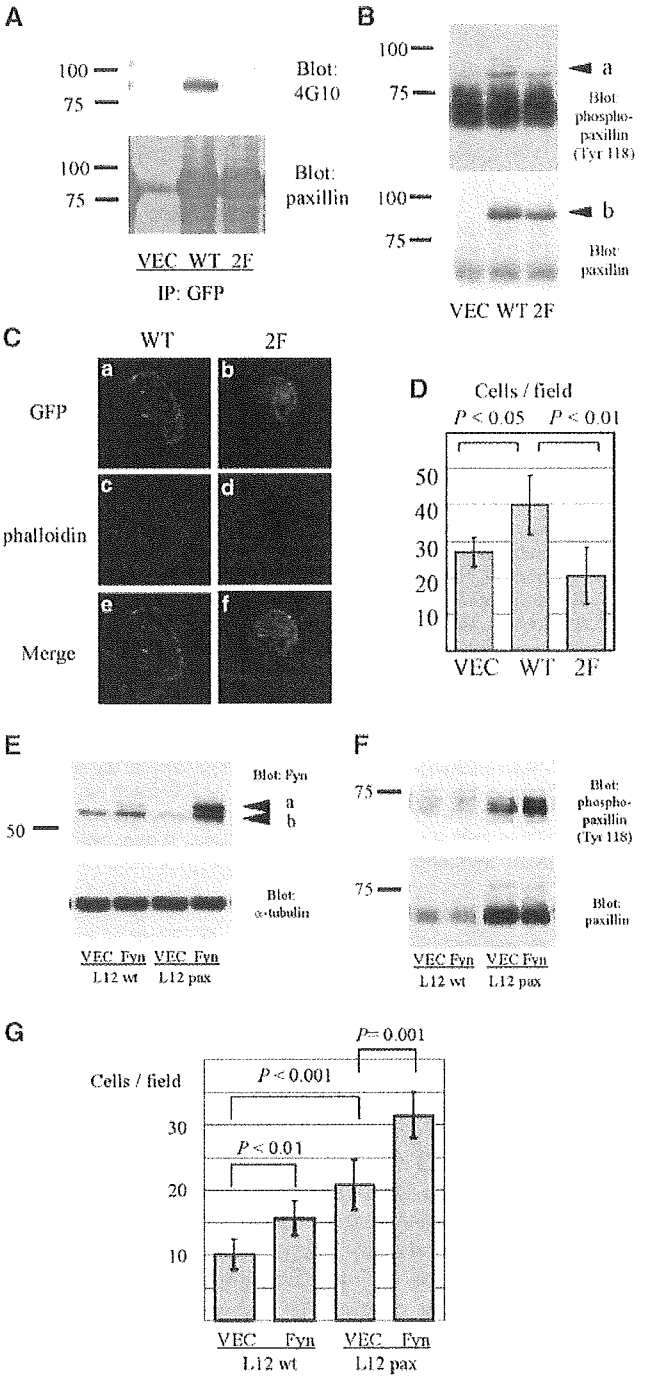

Figure 6 Overexpression of paxillin and elevation of Src family kinase activity synergistically enhance the motility of human osteosarcoma. (**A**) Cos-7 cells were transiently transfected with empty vector (VEC), GFP-paxillin (WT) or GFP-2F (Y31F, Y118F) mutant (2F). Cells were lysed at 48 h from the transfection and immunoprecipitated with anti-GFP antibody. Immunoprecipitates were subjected to immunoblotting analysis by anti-phosphotyrosine antibody 4G10 and anti-paxillin antibody. (**B**) L12 cells were transiently transfected with empty vector (VEC), GFP-paxillin (WT) or GFP-2F mutant (2F). Whole-cell lysates were immunoblotted for anti-phospho-paxillin antibody (Tyr 118) and paxillin antibody. GFP-paxillin and GFP-2F mutant were indicated (arrowhead a and b). (**C**) L12 cells transfected with GFP-paxillin or GFP-2F mutant were chemically stained with phalloidin. GFP (a, b: green) and phalloidin (c, d: red) were visualized with confocal microscopy. (**D**) L12 cells transfected with empty vector, GFP-paxillin or GFP-2F mutant were subjected to migration assay as described in Materials and methods. (**E**, **F**) L12 cells (L12 wt) or paxillin-FLAG-expressing stable cells (L12 pax) were transiently transfected with empty vector (VEC) or Fyn-FLAG (Fyn). Whole-cell lysates were immunoblotted for the antibodies indicated. Fyn-FLAG (arrowhead a) and endogenous Fyn (arrowhead b) were shown in (**E**) upper panel. (**G**) L12 cells or paxillin-FLAG-expressing stable cells that were transiently transfected with empty vector or Fyn-FLAG were subjected to migration assay as described in Materials and methods

Cell motility was enhanced by the transient expression of GFP-paxillin compared with the transfection of GFP-2F mutant or empty vector (Figure 6D). This indicates that the amount of wild-type paxillin is positively correlated with the motility of osteosarcoma sublines. Considering that GFP-2F mutant could localize at focal adhesions (Figure 6C), the lack of motility-promoting effect of GFP-2F mutant was due to the absence of phosphorylation at Tyr 31 and Tyr 118.

The synergistic effect of paxillin overexpression and Src family kinase activity was examined using a low-metastatic subline, L12. We established L12 cells that stably express more than five times as much an amount of exogenous paxillin as the wild-type L12 subline, which is a similar level of endogenous paxillin in the high-metastatic sublines. FLAG epitope-tagged Fyn was transiently transfected to wild-type L12 cells and paxillin-overexpressing L12 cells (Figure 6E). Enhancement of tyrosine phosphorylation of paxillin was observed in Fyn-FLAG-transfected cells compared with mock-transfected cells in both wild-type L12 and paxillin-overexpressing L12 cells (Figure 6F). Cell migration assay reveals that over-expression of both Fyn-FLAG and paxillin-FLAG significantly enhances the cell motility of L12 cells (Figure 6G). This result of cell migration was correlated with the amount of phospho-paxillin in the cells (Figure 6F, upper panel), which suggests that over-expression of paxillin and Fyn contributes to the enhanced motility through the tyrosine phosphorylation of paxillin.

Discussion

We have shown the general enhancement of tyrosine phosphorylation in high-metastatic HuO9 sublines, and the elevated activation of Src family kinase. Among the substrates of Src family kinase, prominent phosphorylation of paxillin along with elevated expression of paxillin was observed in the high-metastatic sublines.

Since human osteosarcoma cell lines suitable for metastatic study were not available, results of previous biochemical analysis on metastatic osteosarcoma were derived from murine models (Khanna *et al.*, 2001, 2004; Iwaya *et al.*, 2003). The present study is the first biochemical analysis on human metastatic osteosarcoma. We used four independent, but genetically close sublines of osteosarcoma that are excellent tools for analysis of signal alteration in the process of acquiring metastatic potential. The high-metastatic sublines were established by *in vivo* selection and the low-metastatic sublines by the dilution plating method. Considering that malignant tumors contain subpopulations of different metastatic capabilities, these selection methods resemble authentic events during the progression of osteosarcoma. Moreover, these sublines were established without any manipulation of genes, which minimizes the artificial effects on our study.

In these sublines of human osteosarcoma, the results of cell motility assay clearly reflected metastatic potential (Nakano *et al.*, 2003). This is reasonable because the properties of cancer cells measured by cell migration assay such as cell movement and ability to interact with extracellular matrix are critical factors during tumor metastasis. Therefore in this study, cell motility was used as an indicator of metastatic potential.

Elevation of Src family kinase activity in metastases was reported in human colorectal cancer (Talamonti *et al.*, 1993) and in human melanoma (Marchetti *et al.*, 1998). According to these reports, there is clear difference in the activated member of Src family kinase among types of tumors. Talamonti *et al.* showed increased activity of c-Src in liver metastases compared to primary tumor. Marchetti *et al.* used brain metastatic sublines and found that kinase activity of Yes, not c-Src, was elevated compared to low-metastatic cells. We recently reported that, in a metastatic model of murine melanoma cell lines, kinase activity of Fyn was elevated in high-metastatic sublines, and interacted with cortactin (Huang *et al.*, 2003). Although not as significant as in the case of murine melanoma, Fyn will also be a candidate for the responsible kinase for metastatic potential of human osteosarcoma. Other members of Src family kinase with relatively low expression, such as c-Src, or with relatively low kinase activity do not appear to be involved in regulation of metastatic potential.

In osteosarcoma, elevated phosphorylation of YDYV motif in $p130^{Cas}$ in high-metastatic sublines (Figure 2a) is a possible clue to Src family activation because phosphorylated YDYV motif in $p130^{Cas}$ stabilizes the active form of Src family kinases by binding with the SH2 domain of Src family kinases (Nakamoto *et al.*, 1996; Burnham *et al.*, 2000). This type of molecule may function as a regulator of Src family kinases that causes activation of Src family kinases in osteosarcoma cells, although the contribution of phosphorylated $p130^{Cas}$ may be low considering the small effect of RNAi on the cell motility.

Although this is the first report on hyperphosphorylation of paxillin in a metastatic tumor, some studies investigated the relationship of cell motility and tyrosine phosphorylation of paxillin. Tyr 31 and Tyr 118 of paxillin are phosphorylated upon cell adhesion (Burridge *et al.*, 1992) and Src family tyrosine kinases (Klinghoffer *et al.*, 1999), FAK (Schaller and Parsons, 1995), and c-Abl (Lewis and Schwartz, 1998) are reported to phosphorylate these sites. The roles of phospho-paxillin on cell motility are still controversial. Migration-promoting effect of phospho-paxillin was demonstrated by using Nara bladder tumor II (NBTII) cells (Petit *et al.*, 2000), while migration-inhibitory effect was shown by using NMuMG cells, MM-1 cells and Cos 7 cells (Yano *et al.*, 2000; Tsubouchi *et al.*, 2002). Our results have added another example of the migration-promoting effects of phospho-paxillin.

The migration-promoting effect of phospho-paxillin might be due to interaction with Crk (Schaller and Parsons, 1995). Crk interacts with a cellular protein DOCK180, which binds directly and activates small GTPase Rac1 (Kiyokawa *et al.*, 1998). Activation of this

pathway provides a link between paxillin–Crk association and cell motility.

The binding partners of phospho-paxillin seem to vary among tumor types and may provide some clue for the controversy between migration-promoting and inhibitory effect of phospho-paxillin. In NMuMG cells, in which phosho-paxillin exerts migration inhibitory effect, phospho-paxillin was shown to bind p120Ras-GAP and RhoA activity was suppressed as a downstream of signal transduction (Tsubouchi *et al*., 2002). Therefore, it is also possible that SH2 domain-containing molecule other than Crk may function as a binding partner of phospho-paxillin and send a positive signal for cell motility in osteosarcoma cells.

We observed the impaired motility by knocking down the expression of paxillin and showed the direct effect of paxillin on cell migration. Paxillin-knocked-down cells showed 67% migration activity compared to LacZ siRNA-treated cells. One reason for this rather weak motility suppression is the partial effect of RNAi, as 40% of paxillin and 68% of phospho-paxillin remained after the treatment with paxillin siRNA compared to LacZ siRNA-treated cells. Another possible reason is the existence of other factors that enhance the metastatic potential independently of paxillin. However, considering the partial effect of RNAi, it can be estimated that paxillin has a significant contribution to high-metastatic phonotype.

We examined the contribution of $p130^{Cas}$, which is another substrate of Src family kinase and involved in the integrin signaling. As a result, suppression of $p130^{Cas}$ expression did not affect the motility of high-metastatic osteosarcoma cells, which supports the relative importance of paxillin in the motility of osteosarcoma cells.

FAK is also known as a binding partner and a substrate of Src family kinase. However, in the osteosarcoma sublines, the tyrosine phosphorylation of FAK was not correlated with the activity of Src family kinase. This may suggest that, in the case of human osteosarcoma, the phosphorylation of FAK reflects other kinase activity including autophosphorylation and is not strongly associated with metastatic potentials.

We have shown the migration-promoting effect of phosho-paxillin by overexpression of GFP-paxillin and its mutant. Expression of exogenous GFP-paxillin enhanced the cell motility in the low-metastatic subline, while expression of GFP-2F mutants did not. Furthermore, we showed paxillin overexpression and Src family activity could contribute to the high metastatic potential of osteosarcoma. Expression of Fyn-FLAG and paxillin-FLAG at the same time in the L12 subline promoted the motility synergistically, although it did not enhance the motility to the extent of high-metastatic sublines, probably because of the existence of other factors which contribute to the high-metastatic potential of osteosarcoma. These results strongly suggest that this cooperative function of Src family kinase and paxillin also works in endogenously expressed proteins and play a major role in high-metastatic phenotype of osteosarcoma cells.

Then, what is the mechanism of overexpression of paxillin in high-metastatic sublines of human osteosarcoma? The locus of paxillin, 17p8q, is not included in the areas where comparative genomic hybridization (CGH) analysis revealed that gene amplification is frequent in human osteosarcoma (Batanian *et al*., 2002; Squire *et al*., 2003; Lau *et al*., 2004). Paxillin mRNA in high-metastatic sublines is at most 1.7 times compared to that in low-metastatic sublines by cDNA microarray analysis (Nakano *et al*., personal communication). Considering high-metastatic sublines express about five times as much paxillin as low-metastatic sublines, paxillin may be highly stable and degraded slowly in high-metastatic sublines.

In conclusion, this study provides information on the importance of phospho-paxillin during metastasis of human osteosarcoma. We have shown that enhancement of Src family kinase activity and overexpression of paxillin synergistically contribute to the high metastatic potential of human osteosarcoma through hyperphosphorylation of paxillin. Further biochemical analysis is needed to clarify the phosphotyrosine-dependent binding partner with paxillin, since the downstream pathway specific to tumor metastasis is a potential therapeutic target. If Src family kinases are activated by a specific mechanism in metastatic osteosarcoma, that would also be an attractive therapeutic target. These themes deserve investigation to improve the extremely poor prognosis of metastatic osteosarcoma.

Materials and methods

Antibodies and reagents

Anti-phosphotyrosine antibody 4G10 was purchased from Upstate Biotechnology. Phospho-specific antibodies against Tyr 460 and Tyr 762 of $p130^{Cas}$ were raised by immunizing rabbits with peptide CAEDVYDVP and CMEDYDYVHL, respectively, and affinity purified. As anti-$p130^{Cas}$ antibody, polyclonal Cas2 antibody was used as described previously (Sakai *et al*., 1994). Monoclonal antibody against FAK was from BD Transduction Laboratories. Polyclonal antibody against phospho-FAK (Tyr 397) was purchased from Upstate Biotechnology. Monoclonal antibody against c-Src (GD11) was from Upstate Biotechnology. Polyclonal antibodies against Fyn (Fyn-3), Fgr (N-47) and pan-Src (Src-2) were from Santa Cruz Biotechnology. Monoclonal antibodies against Yes, Hck, Lck and Lyn were purchased from BD Transduction Laboratories. Monoclonal antibody against paxillin was from Zymed Laboratories Inc. Polyclonal antibody against phospho-paxillin (Tyr 118) was purchased from Cell Signaling. Anti-α-tubulin antibody (B-5-1-2) was purchased from SIGMA. Monoclonal antibody against Abl was from BD Biosciences. Polyclonal antibody against GFP (598B) was from Medical and Biological Laboratories. HRP-conjugated anti-mouse antibody was purchased from Amersham Pharmacia. Alexa Fluor 488 goat anti-mouse IgG, Alexa Fluor 594 goat anti-rabbit IgG and Alexa Fluor 546 phalloidin were purchased from Molecular Probe. Normal rabbit serum was from DakoCytomation. Src family kinase inhibitor PP2 and the structural analog PP3 were purchased from Calbiochem-Novabiochem Ltd.

Plasmids

A FLAG epitope-tagged paxillin construct was generated by amplifying the coding sequence of human paxillin by PCR using the primers 5′-CGTACCTCGAGGCCATGGACGA CCTCGACGC-3′ and 5′-GGAATTCATTTGTCGTCGTC GTCCTTGTAGTCGCAGAAGAGCTTGAGGAAGC-3′. This resulted in a fragment with an *Xho*I site (underlined), a sequence encoding the FLAG epitope (DYKDDDDK), followed by a termination codon and an *Eco*RI site (underlined). This fragment was then digested with *Xho*I and *Eco*RI sequentially, and ligated into the mammalian expression vector pcDNA3.1(−)/ Myc-His B (Invitrogen).

GFP-paxillin is a kind gift from Dr Y Sawada (Department of Biological Sciences, Columbia University). Phenylalanine mutant at Tyr 31 and Tyr 118 was generated by amplifying GFP-paxillin with following primers. 5′-CGGCCTGTGT TCTTAAGCGAGGAGACCCCCTTCTCATACCCAAC-3′ and 5′-GTTGGGTATGAGAAGGGGGTCTCCTCGCTTA AGAACACAGGCCG-3′ were used for Tyr 31, and 5′-CCGTGCTCTAGAGTGGGAGAGGAGGAGCACGTGT TCAGCTTCCC-3′ and 5′-GGGAAGCTGAACACTGTC TCCTCCTCTCCCACTCTAGAGCACGG-3′ were used for Tyr 118.

A FLAG epitope-tagged Fyn construct was generated by amplifying the RT–PCR product of human colon cancer cell line, HCT116, by PCR using the primers 5′-GGATC CATGGGCTGTGTGCAATGTAAG-3′ and 5′-GTTAACT CACTTGTCGTCATCGTCCTTGTAGTCCAGGTTTTCA CCAGGTTG-3′. This PCR product was first inserted into pGEM-T Easy vector (Promega), followed by excision with *Eco*RI, and ligated into the mammalian expression vector pcDNA3.1(−)/Myc-His A (Invitrogen).

Cell culture and transfection

A human osteosarcoma cell line, HuO9, and its high-metastatic (M112, M132) and low-metastatic (L12, L13) sublines have been described previously (Nakano *et al*., 2003). Osteosarcoma cells were maintained in RPMI 1640 medium with 10% fetal bovine serum (FBS) at 37°C with 5% CO_2. Cos-7 cells were maintained in Dulbecco's modified Eagle's medium (DMEM) with 10% FBS at 37°C with 5% CO_2. Transfection was performed by using FuGENE 6 (Roche) according to the manufacturer's instruction. Selection of clones was performed by using geneticin (Sigma) at the concentration of 30 μg/ml.

Immunoblotting and immunoprecipitation

Before extracting cell lysates, osteosarcoma cells were cultured for at least 48 h to ensure complete cell adhesion to culture dishes unless otherwise indicated. Cells were lysed in 1% Triton X-100 buffer (50 mM HEPES, 150 mM NaCl, 10% glycerol, 1% Triton-X 100, 1.5 mM $MgCl_2$, 1 mM EGTA, 100 mM NaF, 1 mM Na_3VO_4, 10 μg/ml aprotinin, 10 μg/ml leupeptin, 1 mM phenylmethylsulfonyl fluoride), and insoluble materials were removed by centrifugation. To investigate the effect of PP2 treatment, cells were treated with 10 μM of PP2 or 10 μM of PP3 for 30 min prior to harvesting cells.

Protein concentration was measured by BCA Protein Assay (PIERCE) and the protein aliquots were separated by SDS–PAGE. Gels were transferred to a polyvinylidene difluoride membrane (Millipore) and subjected to immunoblotting. After blocking in 5% skim milk/TBST (100 mM Tris-HCl pH 8.0, 150 mM NaCl, 0.05% Tween 20) for 1 h, blots were incubated with appropriate primary antibodies. In case of 4G10 stain, blocking was performed with 5% bovine serum albumin (BSA) which was used instead of skim milk. Blots were then washed three times with TBST, incubated with HRP-conjugated secondary antibodies for 30 min, washed twice by TBST and twice with TBS (100 mM Tris-HCl pH 8.0, 150 mM NaCl), and visualized by autoradiography using chemiluminescence reagent (Western Lighting, Perkin Elmer).

The images were captured by molecular imager GS800 (BIO-RAD) and the density of each smear was quantified by Quantity One (BIO-RAD).

For immunoprecipitation, aliquots of protein were mixed with appropriate antibodies and incubated for 1 h on ice. Then, samples were rotated with protein A- or protein G-sepharose beads (Amersham Pharmacia) for 2–12 h at 4°C. After the beads were washed four times with 1% Triton-X 100 buffer, the samples were boiled in sample buffer (0.1 M Tris-HCl pH 6.8, 2% SDS, 0.1 M dithiothreitol, 10% glycerol, 0.01% bromophenol blue) for 5 min and analysed by SDS–PAGE.

Immunocytochemistry

Cells were grown on 12-mm circle cover glasses (Fisher) in 24-well plates, washed three times with phosphate-buffered saline (PBS), fixed with 4% paraformaldehyde/0.1 M phosphate buffer for 5 min at room temperature, washed once with PBS, and permeabilized with 0.2% Triton-X 100 in PBS for 10 min. After another washing step with PBS and blocking in 5% goat serum and 3% BSA/TBST for 30 min, cells were incubated with anti-paxillin antibody (1 : 2000) and anti-phospho-paxillin antibody (1 : 250) in 5% goat serum and 3% BSA/TBST for 1 h at room temperature. Cells were washed three times with PBS and incubated with appropriate second antibodies (Molecular Probe) (1 : 2000) in 5% goat serum and 3% BSA/TBST. When actin was stained with phalloidin, Alexa Fluor phalloidin was combined with second antibody at the concentration of 1 U/ml.

After cells were washed three times with PBS, cover glasses were mounted in 1.25% DABCO, 50% PBS, 50% glycerol and visualized using a Radiance 2100 confocal microscopic system (BIO-RAD).

In vitro *kinase assay*

For kinase assay, fresh cell lysate was prepared and mixed with the antibody of interest for 1 h on ice. Then, samples were rotated with protein A-sepharose or protein G-sepharose for 1 h at 4°C. The beads were consequently washed with 1% Triton-X 100 buffer and kinase buffer (50 mM Tris HCl, pH 7.4, 50 mM NaCl, 10 mM $MgCl_2$, 10 mM $MnCl_2$) three times, respectively. Kinase reaction was performed in 30 μl of kinase buffer with 10 μg of synthetic polypeptides poly[Glu-Tyr](4 : 1) (Sigma) as exogenous substrate and 5 μCi of [γ-32P]ATP (ICN) at room temperature for 1 h. Kinase reaction was stopped by the addition of SDS–PAGE sample buffer (0.1 M Tris-HCl pH 6.8, 2% SDS, 0.1 M dithiothreitol, 10% glycerol, 0.01% bromophenol blue). The samples were boiled for 5 min and analysed by SDS–PAGE using 8% polyacrylamide gel. The gels were then dried and exposed to autoradiography. The images were captured by molecular imager GS800 (BIO-RAD) and the density of each smear (area shown by a bracket) was quantified by Quantity One (BIO-RAD).

Cell migration assay

Cell migration assay was performed by using Cell Culture Insert with 8.0 μm pore size PET filter (Becton Dickinson). Prior to the assay, the lower surface of the filter was immersed for 30 min in 10 μg/ml fibronectin (Sigma) diluted with PBS. Next, 700 μl of RPMI 1640 medium with 10% FCS was added to the lower chamber. Then, 5×10^4 cells were suspended in 300 μl of RPMI 1640 medium with 10% FCS and added to the upper chamber.

After incubation for 24 h at 37°C in a humid 5% CO_2 atmosphere, the cells on the upper surface of the filter were completely removed by wiping with cotton swabs. The cells on the lower surface of the filter were fixed in methanol for 30 min, washed with PBS, and then stained with Giemsa's stain solution (Muto Pure Chemicals Co. Ltd.) for 30 s. After washing three times with PBS, the filters were mounted on a glass slide. The cells on the lower surface were counted from photographs taken of at least five fields at a magnification of $\times 200$ under the microscope. Student's *t*-test was used to analyse data from these experiments. To investigate the effect of PP2 treatment, cells were allowed to migrate in the presence of 10 μM of PP2 or 10 μM of PP3.

RNAi analysis

siRNA of human paxillin and $p130^{Cas}$ was generated using BLOCK-iT RNAi TOPO Transcription Kit and BLOCK-iT Complete Dicer RNAi Kit (Invitrogen) according to the manufacturer's instructions. In the generation of siRNA for paxillin, 936 bp from the initiation codon of human paxillin were chosen as the target sequence, and amplified by PCR using the primers, 5′-ATGGACGACCTCGACGCC-3′ and 5′-GTTCAGGTCAGACTGCAGGC-3′. As for $p130^{Cas}$, 866 bp was chosen as the target sequence, and amplified with the primers, 5′-ACACCATGAACCACCTGAACGTG-3′ and 5′-ATACACCTCCAGCAACGGGT-3′.

siRNA of LacZ was generated in the same procedure as paxillin siRNA, and was used as a negative control. Transfection was performed with Lipofectamine 2000 (Invitrogen) and the effect was analysed 72 h after the transfection.

Abbreviations

BSA, bovine serum albumin; Cas, Crk-associated substrate; FAK, focal adhesion kinase; FBS, fetal bovine serum; PBS, phosphate-buffered saline; PP2, 4-amino-5-(4-chlorophenyl)-7-(t-butyl)pyrazolo[3,4-d]pyrimidine; PP3, 4-amino-7-phenylpyrazol [3,4-d]pyrimidine; RNAi, RNA interference; SH2, Src homology 2 domain; siRNA, short interfering RNA.

Acknowledgements

We are grateful to Dr Y Sawada (Department of Biological Sciences, Columbia University) for donating paxillin cDNA. KA is an awardee of the Research Resident Fellowship from the Foundation for Promoting of Cancer Research (Japan) for the 3rd Term Comprehensive 10-Year-Strategy for Cancer Control. This study was supported by the Program for Promotion of Fundamental Studies in Health Science of Pharmaceuticals and Medical Devices Agency (PMDA).

References

Batanian JR, Cavalli LR, Aldosari NM, Ma E, Sotelo-Avila C, Ramos MB, Rone JD, Thorpe CM and Haddad BR. (2002). *Mol. Pathol.*, **55,** 389–393.

Burnham MR, Bruce-Staskal PJ, Harte MT, Weidow CL, Ma A, Weed SA and Bouton AH. (2000). *Mol. Cell. Biol.*, **20,** 5865–5878.

Burridge K, Turner CE and Romer LH. (1992). *J. Cell. Biol.*, **119,** 893–903.

Huang J, Asawa T, Takato T and Sakai R. (2003). *J. Biol. Chem.*, **278,** 48367–48376.

Huth JF and Eilber FR. (1989). *Arch. Surg.*, **124,** 122–126.

Iwaya K, Ogawa H, Kuroda M, Izumi M, Ishida T and Mukai K. (2003). *Clin. Exp. Metast.*, **20,** 525–529.

Khanna C, Khan J, Nguyen P, Prehn J, Caylor J, Yeung C, Trepel J, Meltzer P and Helman L. (2001). *Cancer Res.*, **61,** 3750–3759.

Khanna C, Wan X, Bose S, Cassaday R, Olomu O, Mendoza A, Yeung C, Gorlick R, Hewitt SM and Helman LJ. (2004). *Nat. Med.*, **10,** 182–186.

Kimura K, Nakano T, Park YB, Tani M, Tsuda H, Beppu Y, Moriya H and Yokota J. (2002). *Clin. Exp. Metast.*, **19,** 477–485.

Kiyokawa E, Hashimoto Y, Kobayashi S, Sugimura H, Kurata T and Matsuda M. (1998). *Genes Dev.*, **12,** 3331–3336.

Klinghoffer RA, Sachsenmaier C, Cooper JA and Soriano P. (1999). *EMBO J.*, **18,** 2459–2471.

Lau CC, Harris CP, Lu XY, Perlaky L, Gogineni S, Chintagumpala M, Hicks J, Johnson ME, Davino NA, Huvos AG, Meyers PA, Healy JH, Gorlick R and Rao PH. (2004). *Genes Chromosomes Cancer*, **39,** 11–21.

Lewis JM and Schwartz MA. (1998). *J. Biol. Chem.*, **273,** 14225–14230.

Marchetti D, Parikh N, Sudol M and Gallick GE. (1998). *Oncogene*, **16,** 3253–3260.

Meyers PA, Heller G, Healey JH, Huvos A, Applewhite A, Sun M and LaQuaglia M. (1993). *J. Clin. Oncol.*, **11,** 449–453.

Nakamoto T, Sakai R, Ozawa K, Yazaki Y and Hirai H. (1996). *J. Biol. Chem.*, **271,** 8959–8965.

Nakano T, Tani M, Ishibashi Y, Kimura K, Park YB, Imaizumi N, Tsuda H, Aoyagi K, Sasaki H, Ohwada S and Yokota J. (2003). *Clin. Exp. Metast.*, **20,** 665–674.

Pawson T. (2004). *Cell*, **116,** 191–203.

Petit V, Boyer B, Lentz D, Turner CE, Thiery JP and Valles AM. (2000). *J. Cell. Biol.*, **148,** 957–970.

Sakai R, Iwamatsu A, Hirano N, Ogawa S, Tanaka T, Mano H, Yazaki Y and Hirai H. (1994). *EMBO J.*, **13,** 3748–3756.

Schaller MD. (2001). *Oncogene*, **20,** 6459–6472.

Schaller MD, Hildebrand JD, Shannon JD, Fox JW, Vines RR and Parsons JT. (1994). *Mol. Cell. Biol.*, **14,** 1680–1688.

Schaller MD and Parsons JT. (1995). *Mol. Cell. Biol.*, **15,** 2635–2645.

Schlaepfer DD, Broome MA and Hunter T. (1997). *Mol. Cell. Biol.*, **17,** 1702–1713.

Squire JA, Pei J, Marrano P, Beheshti B, Bayani J, Lim G, Moldovan L and Zielenska M. (2003). *Genes Chromosomes Cancer*, **38,** 215–225.

Talamonti MS, Roh MS, Curley SA and Gallick GE. (1993). *J. Clin. Invest.*, **91,** 53–60.
Tsubouchi A, Sakakura J, Yagi R, Mazaki Y, Schaefer E, Yano H and Sabe H. (2002). *J. Cell. Biol.*, **159,** 673–683.
Tsuchiya H, Kanazawa Y, Abdel-Wanis ME, Asada N, Abe S, Isu K, Sugita T and Tomita K. (2002). *J. Clin. Oncol.*, **20,** 3470–3477.
Turner CE. (2000). *Nat. Cell. Biol.*, **2,** E231–E236.
Ward WG, Mikaelian K, Dorey F, Mirra JM, Sassoon A, Holmes EC, Eilber FR and Eckardt JJ. (1994). *J. Clin. Oncol.*, **12,** 1849–1858.
Yano H, Uchida H, Iwasaki T, Mukai M, Akedo H, Nakamura K, Hashimoto S and Sabe H. (2000). *Proc. Natl. Acad. Sci. USA*, **97,** 9076–9081.
Yeatman TJ. (2004). *Nat. Rev. Cancer*, **4,** 470–480.

Supplementary Information accompanies the paper on Oncogene website (http://www.nature.com/onc)

14

Immunohistochemical Detection of EBAG9/RCAS1 Expression in Hepatocellular Carcinoma

Taku Aoki, Hiroshi Imamura, Masatoshi Makuuchi, and Satoshi Inoue

Introduction

Identification of EBAG9/RCAS1

Estrogen receptor–binding fragment-associated gene 9 (*EBAG9*) is an estrogen-responsive gene that has been isolated from a CpG island library of MCF-7 human breast cancer cells by the genomic binding-site cloning method (Watanabe *et al.*, 1998). The complementary deoxyribonucleic acid (cDNA) of human EBAG9 encodes an open reading frame (ORF) of 213 amino acids. An estrogen-responsive element (ERE) is located in the 5′ flanking region of the EBAG9 gene, and its transcript is directly up-regulated by estrogen (Tsuchiya *et al.*, 2001; Watanabe *et al.*, 1998).

The receptor-binding cancer antigen expressed on SiSo cells (RCAS1) was originally isolated as the antigen recognized by 22-1-1 antibody against human uterine adenocarcinoma cell line SiSo (Sonoda *et al.*, 1996) and was later found to be identical to EBAG9 (EBAG9/RCAS1) (Nakashima *et al.*, 1999). Based on *in vitro* observation, RCAS1 has been assumed to act as a ligand for a putative receptor present on normal peripheral lymphocytes, such as T, B, and natural killer (NK) cells. RCAS1 has also been found to inhibit the growth of activated $CD3^+$ T lymphocytes and NK cells and to induce apoptotic cell death (Nakashima *et al.*, 1999). Based on these observations, it has been speculated that EBAG9/RCAS1 is involved in the escape of tumor cells from immune system action.

EBAG9/RCAS1 Expression in Normal Tissue and Cancer Tissue

Two antibodies have been used to assess the expression of EBAG9/RCAS1 in various tissues and cell lines. The first is the 22-1-1 monoclonal antibody established by cell fusion between mouse myeloma cells and spleen cells derived from mice immunized with human uterine cervical adenocarcinoma cell line, SiSo (Sonoda *et al.*, 1996). Immunoreactivity to this antibody has been detected in normal human tissues, such as uterine endometrial glands (Sonoda *et al.*, 2000), goblet cells of bronchi and bronchioles (Iwasaki *et al.*, 2000; Izumi *et al.*, 2001), and gastric mucosa (Kubokawa *et al.*, 2001). Immunoreactivity has also been reported in various cancer tissues, including cancer of the uterus (Kaku *et al.*, 1999; Sonoda *et al.*, 1996; Sonoda *et al.*, 1998; Sonoda *et al.*, 2000), ovary (Sonoda *et al.*, 1996), lung (Iwasaki *et al.*, 2000; Izumi *et al.*, 2001; Oizumi *et al.*, 2002), stomach (Kubokawa *et al.*, 2001), skin (Takahashi *et al.*, 2001), gallbladder (Oshikiri *et al.*, 2001), esophagus (Nakakubo *et al.*, 2002), pancreas (Hiraoka *et al.*, 2002), bile duct

Handbook of Immunohistochemistry and *in situ* Hybridization of Human Carcinomas, Volume 3: Molecular Genetics, Liver Carcinoma, and Pancreatic Carcinoma

(Enjoji *et al.*, 2002; Suzuoki *et al.*, 2002), and liver (Noguchi *et al.*, 2001).

We raised a rabbit polyclonal anti-EBAG9 antibody against a glutathione-*S*-transferase (GST)-EBAG9 fusion protein (Tsuchiya *et al.*, 2001), and the antibody has been shown to react with human and mouse EBAG9 and yield a 32-kD band in Western Blot analysis. The intensity of the band has been shown to be reduced by prior incubation of the antibody with recombinant EBAG9 protein (Suzuki *et al.*, 2001). Immunostaining with this polyclonal antibody has shown that EBAG9 is expressed in various tissues from normal mice, including liver (Tsuchiya *et al.*, 2001), and tissues from normal humans, such as mammary gland tissue (Suzuki *et al.*, 2001) and prostate tissue (Takahashi *et al.*, 2003). EBAG9 has also been shown to be widely distributed in human breast cancer and prostate cancer (Suzuki *et al.*, 2001; Takahashi *et al.*, 2003).

Because the reports referred to earlier have documented that expression of EBAG9/RCAS1 is more remarkable in cancer tissues than in normal tissues, EBAG9/RCAS1 has attracted attention as a potential cancer-associated antigen. Its expression is generally thought to be related to tumor invasiveness and to be associated with poor patient prognosis in cancer of the uterus (Kaku *et al.*, 1999), lung (Iwasaki *et al.*, 2000; Izumi *et al.*, 2001; Oizumi *et al.*, 2002), gallbladder (Oshikiri *et al.*, 2001), esophagus (Nakakubo *et al.*, 2002), pancreas (Hiraoka *et al.*, 2002), bile duct (Suzuoki *et al.*, 2002), and prostate (Takahashi *et al.*, 2003).

Stepwise Evolution of Hepatocellular Carcinoma and EBAG9/RCAS1 Expression in Hepatocellular Carcinoma

Hepatocellular carcinoma (HCC) is one of the most common malignancies worldwide, ranking 5th in frequency in the world (Parkin *et al.*, 2001). Although HCC is more prevalent in Asia and Africa, its incidence is on the rise in Western countries (El-Serag and Mason, 1999; El-Serag *et al.*, 2003; Taylor-Robinson *et al.*, 1997). The condition HCC has the unique characteristic of developing and progressing in a typical multistep manner—that is, from early HCC (Liver Cancer Study Group of Japan, 2000; Takayama *et al.*, 1998), through early-advanced HCC, to advanced HCC (Kojiro and Nakashima, 1999). Most early HCCs are small, well-differentiated nodules with low proliferative activity, but when they progress to a more advanced stage, they transform into moderately to poorly differentiated cancers and undergo a rapid increase in size. During this process (tumor dedifferentiation and proliferation), HCCs acquire malignant potential as reflected by intrahepatic metastasis and vascular invasion (see later discussion). This transformation occurs non-uniformly within a given tumor nodule, resulting in the simultaneous presence of well-differentiated and moderately to poorly differentiated lesions within the same nodule. This produces what histologists refer to as a "nodule-in-nodule" or "mosaic" appearance (Kojiro and Nakashima, 1999). As mentioned earlier, HCC frequently invades blood vessels, especially the portal system, resulting in intrahepatic metastasis. Many previous reports have documented vascular invasion and intrahepatic metastasis as unfavorable prognostic factors.

In this chapter, we describe immunohistochemical detection of EBAG9/RCAS1 expression in noncancerous liver tissue and in HCC tissue, especially the methodologic aspects. We used a rabbit polyclonal anti-EBAG9 antibody (Tsuchiya *et al.*, 2001). In view of the pathologic features of HCC and the results of previous studies on EBAG9/RCAS1 as a cancer marker, we paid particular attention to the multistep evolution of HCC, including the following: 1) process of tumor dedifferentiation, 2) cancer proliferative activity, and 3) ability to metastasize. The overall results have previously been reported by our group elsewhere (Aoki *et al.*, 2003).

MATERIALS

Liver Samples

Samples of HCC tissue and adjacent noncancerous liver tissue from 143 cases of HCC were analyzed immunohistochemically. Testing for hepatitis B virus surface antigen was positive in 23 patients, and testing for anti-hepatitis C virus (HCV) antibody was positive in 100 patients. The liver tissue was obtained during surgery in our department between October 1994 and December 1998. Ten liver biopsy specimens obtained for preoperative evaluation of potential liver transplant donors, and 10 liver biopsy specimens obtained to assess patients who were serologically anti-HCV antibody positive were also made available for the analysis as noncancerous samples. The biopsy specimens from the patients who were HCV antibody positive were kindly provided by Dr. Jyunichi Fukushima (Department of Pathology, Teikyo University School of Medicine, Tokyo, Japan).

Materials for Immunohistochemistry

1. 10% formalin for fixation.
2. Xylene: for dewaxing.
3. Ethanol: diluted to 50%, 70%, 90%, and 95% with distilled water.

4. Tris-buffered saline (TBS): 6.06 g TRIZMA Base and 8.77 g NaCl; brought to a volume of 1 L with deionized distilled water and adjusted to pH 7.6 with HCl.

5. 10 mM Na-citrate solution (pH 6.0): 2.10 g citric acid brought to a volume of 1 L with deionized distilled water and adjusted to pH 6.0 with 6 M NaOH.

6. 0.3% hydrogen peroxide (H_2O_2) in 100% methanol: 150 ml of 100% methanol was mixed with 1.5 ml of 30% H_2O_2.

7. Fetal calf serum (FCS): stored at –20°C.

8. Primary antibody: rabbit polyclonal anti-EBAG9 antibody (Tsuchiya *et al.*, 2001) diluted 1:40 in 10% FCS-TBS or normal rabbit immunoglobulin (IgG) diluted 1:800 in 10% FCS-TBS.

9. Envision (Dako, Glostrup, Denmark; for rabbit polyclonal antibody).

10. 3,3′-diaminobenzidine tetrahydrochloride (DAB) working solution mixed with Tris-HCl (pH 7.5) and 0.02% H_2O_2.

11. 50% Mayer's hematoxylin: for counterstaining.

METHOD

Liver Tissue Preparation

Resected liver specimens were fixed in 10% formalin, cut into blocks, and embedded in paraffin. They were then sliced into 4-μm sections and mounted on glass slides.

Protocol for EBAG9/RCAS1 Immunostaining

1. Dip the slides in xylene for 3 min 3×.
2. Dip the slides in 100% ethanol for 3 min 2×.
3. Dip the slides in 95% ethanol for 3 min 2×.
4. Rinse the slides in TBS for 5 min.
5. Dip the slides in 10 mM Na-citrate solution (pH 6.0) and then heat them in an autoclave at 125°C for 5 min.
6. Rinse the slides in TBS for 5 min. at room temperature.
7. Block endogenous peroxide by dipping the slides in 0.3% hydrogen peroxide (H_2O_2) in 100% methanol for 30 min.
8. Rinse the slides in TBS for 5 min 3×.
9. Block nonspecific binding by incubating the sections in 10% FCS-TBS for 30 min in a moist chamber.
10. Incubate the sections in primary antibody (rabbit polyclonal antibody for EBAG9) or control rabbit IgG diluted in 10% FCS-TBS in a moist chamber at 4°C overnight.
11. Wash the slides quickly in TBS 3× at room temperature.
12. Rinse the slides in TBS for 5 min.
13. Incubate the sections in Envision (Dako; for rabbit polyclonal antibody) for 1 hr in a moist chamber at room temperature.
14. Rinse the slides in TBS for 5 min 3× at room temperature.
15. Visualize the staining with 3,3′-DAB: apply the working solution and stop the reaction as soon as adequate color develops (usually 2–3 min).
16. Counterstain the sections in 50% Mayer's hematoxylin.
17. Wash the slides in tap water for 5 min.
18. Dip the slides in graded ethanol solutions (50%, 70%, 90%, and 100%) and then in xylene (each for 3 min).
19. Place coverslips on the sections. They are now ready for final examination under a light microscope.

RESULTS AND DISCUSSION

EBAG9 Expression in Normal and Chronically Diseased Liver

Noncancerous hepatocytes, including hepatocytes from normal liver, chronic HCV-related hepatitis, or cirrhotic liver, displayed a low but significant level of EBAG9 immunoreactivity (Figure 43a). High-power magnification revealed punctate staining concentrated specifically near the cell membrane bordering adjacent hepatocytes (not shown). The distribution of the EBAG9 staining was homogeneous and regular throughout the tissue, suggesting that it becomes localized in the cells.

EBAG9/RCAS1 has been detected in various normal human tissues, e.g., uterine endometrial glands (Sonoda *et al.*, 2000), goblet cells of bronchi and bronchioles (Iwasaki *et al.*, 2000; Izumi *et al.*, 2001), mammary glands (Suzuki *et al.*, 2001), and gastric mucosa (Kubokawa *et al.*, 2001), suggesting that EBAG9/RCAS1 is expressed and secreted by gland cells. Thus, the polarity of EBAG9/RCAS1 expression in noncancerous liver tissue suggests that it is related to some physiologic function, e.g., glandular secretion, in normal liver tissue.

EBAG9 Expression in Hepatocellular Carcinoma

EBAG9 Expression at the Cell Level

The EBAG9 immunoreactivity of HCC cells varied. Some exhibited weak immunoreactivity, similar to that of noncancerous hepatocytes (enhancement-negative cells) (Figure 43b), whereas others displayed enhanced immunoreactivity (enhancement-positive cells)

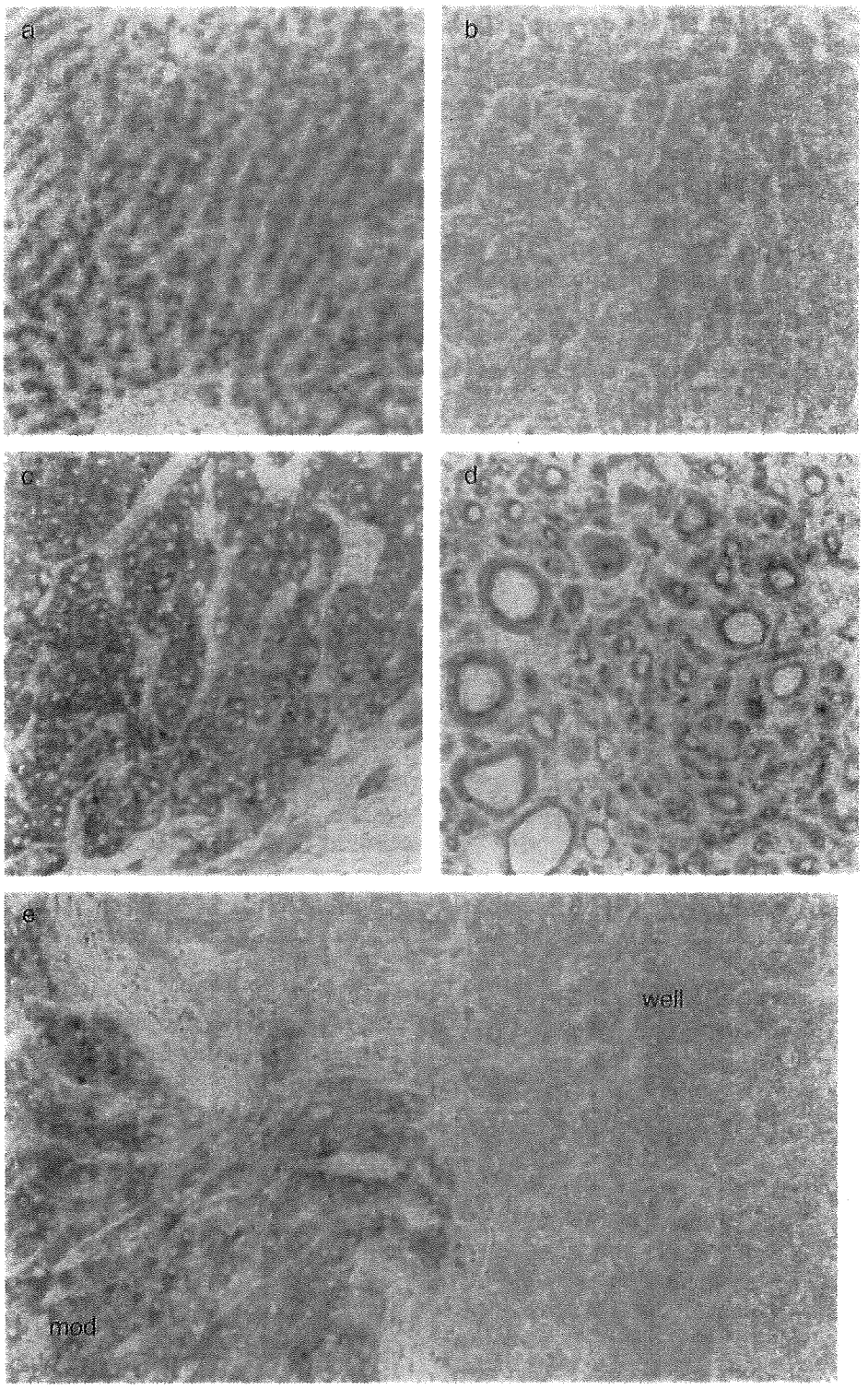

Figure 43. a: Normal liver tissue showing weak EBAG9 immunoreactivity. The staining pattern is homogeneous and regular throughout the tissue (200X). **b:** A well differentiated hepatocellular carcinoma (HCC) classified as EBAG9-negative. The pattern of expression is similar to the pattern in noncancerous tissue (200X). **c:** An EBAG9-positive case of moderately differentiated HCC (trabecular type) (200X). Immunoreactivity is detected over the entire surface of the cancer cells and in their cytoplasm. **d:** Pseudoglandular type of moderately differentiated HCC displaying intense expression on the apical surface of the cells (200X). **e:** A tumor with a "nodule-in-nodule" appearance showing intense staining in the interior, moderately differentiated region ("mod"), contrasting with weak staining in the outer, well-differentiated region ("well") (100X).

(Figure 43c). The staining pattern in enhancement-negative cancer cells showed regular distribution of EBAG9-positive granules, similar to the pattern in noncancerous hepatocytes. By contrast, in the majority of enhancement-positive cells there was intense staining over the entire surface of the cell as well as in the cytoplasm. Coarse, thickened granules were dispersed throughout the cytoplasm, and the regularity of the granule distribution noted in the noncancerous hepatocytes was lost. This finding was consistent with observations in the cells of invasive ductal carcinoma of the breast showing that normal mammary gland cells expressed EBAG9/RCAS1 only on their apical surface, whereas carcinoma cells exhibit enhanced expression without a polar distribution (Suzuki *et al.*, 2001). The apical surfaces of the pseudoglands stained strongly in the pseudoglandular type of moderately differentiated HCC (Figure 43d).

Intranodular Distribution of Enhanced EBAG9 Immunoreactivity

The proportion and distribution of enhancement-positive cancer cells were highly variable from nodule to nodule (range 5–100%). It is interesting that, "nodule-in-nodule" tumors, i.e., those consisting of a combination of well-differentiated lesion and a less-differentiated lesion, displayed different immunoreactivity in the two regions, with the less-differentiated intensely immunoreactive region contrasting clearly with the weakly immunoreactive well-differentiated region (Figure 43e).

Semiquantitative Classification of EBAG9 Expression in Hepatocellular Carcinoma Sections

Based on the observations described earlier, HCC section was classified in a semiquantitative manner as follows:

1. Negative (−): sections in which all the cancer cells were identified as enhancement-negative.
2. Borderline (±): sections in which 1–5% of the malignant cells were enhancement-positive, or, sections showing uniformly positive but very weak immunoreactivity.
3. Positive (+): sections in which more than 5% of enhancement-positive cancerous cells.

As a result, 35 of the 143 sections examined (24.5%) were classified as negative, 24 (16.8%) as borderline, and 84 (58.7%) as positive.

Correlation between EBAG9 Expression and Pathologic Variables

For purposes of analysis, the borderline group and negative group were combined and compared with the positive group. The relationship between EBAG9 immunoreactivity and various clinicopathologic parameters was analyzed by comparing the EBAG9-positive group (n = 84) with the EBAG9-negative/borderline group (n = 59), as shown in Table 17. Enhanced EBAG9 immunoreactivity was more frequently observed in the less-differentiated tumors (P = 0.01), and EBAG9 immunoreactivity was significantly correlated with the Ki-67 labeling index. However, there was no significant correlation between enhanced EBAG9 expression and tumor invasiveness (Kosuge *et al.*, 1993; intrahepatic metastasis and/or vascular invasion) (P = 0.86). No other clinical or pathologic variables were significantly correlated with enhanced EBAG9 expression, and no significant correlation was established between enhanced EBAG9 expression and disease-free survival evaluated by the Kaplan-Meier method and log-rank test (P = 0.17) (Figure 44).

EBAG9/RCAS1 Expression in the Process of Stepwise Hepatocellular Carcinoma Progression

Our results showed that enhanced EBAG9/RCAS1 expression is closely correlated with degree of tumor differentiation and increased Ki-67 labeling index. Ki-67 is now widely used as a marker of cell proliferation, including in human studies (Gerdes *et al.*, 1984; Scholzen and Gerdes, 2000). Thus, our findings suggest that enhanced EBAG9/RCAS1 expression is associated with HCC tumor progression as represented by dedifferentiation and proliferation. It is interesting that, tumors showing a "nodule-in-nodule" appearance displayed intense expression in the less-differentiated region and weak expression in the more highly differentiated region (Figure 43e), suggesting that enhancement of EBAG9/RCAS1 expression parallels tumor dedifferentiation.

In contrast to a previous report (Noguchi *et al.*, 2001), EBAG9/RCAS1 was unassociated with tumor metastasis in our series. All of our results lead us to conclude that EBAG9/RCAS1 is closely associated with tumor dedifferentiation and proliferation but not with tumor metastasis. In other words, EBAG9/RCAS1 appears to be more related to growth of the primary tumor than to development of tumor metastases. Our results therefore imply that enhanced EBAG9/RCAS1 expression is an intermediate event in the multistep progression of HCC and is unrelated to the final event, which is characterized by the frequent occurrence of vascular invasion and resultant intrahepatic metastasis. Because enhanced EBAG9 expression was not significantly associated with patient disease-free survival, EBAG9 may not be a prognostic factor in patients with HCC. Nevertheless, we consider it to be of value as a